**NASA Technical Paper 2886**
**DOT/FAA/DS-89/06**

1989

# Piloted-Simulation Evaluation of Recovery Guidance for Microburst Wind Shear Encounters

David A. Hinton
*Langley Research Center*
*Hampton, Virginia*

National Aeronautics and Space Administration
Office of Management
Scientific and Technical Information Division

## Summary

Numerous air carrier accidents and incidents have resulted from inadvertent encounters with the atmospheric wind shear associated with microburst phenomena, in some cases resulting in a heavy loss of life. The Federal Aviation Administration and the National Aeronautics and Space Administration (NASA) are addressing the wind shear hazard through the Integrated Wind Shear Program. The goal of the plan is to reduce the hazard of low-level wind shear to aircraft through improved airborne and ground-based wind shear detection systems, crew alerting and flight guidance systems, and training and operating procedures. NASA is investigating the airborne aspects of the problem through hazard characterization, sensor technology, and flight management systems. This study addresses the recovery strategies that may be implemented by future flight management systems.

Although the ultimate objective of the wind shear program is to permit airplanes to avoid encounters with severe wind shear, an important issue is how airplane performance can be managed best during an inadvertent wind shear encounter. The goals of this study were (1) to develop techniques and guidance for maximizing the ability of the airplane to recover from microburst encounters, (2) to develop an understanding of how theoretical predictions of wind shear recovery performance might be achieved in actual use, and (3) to gain insight into the piloting factors associated with recovery from microburst encounters. Only the case of wind shear encounter at takeoff was considered. Three recovery strategies, developed in a related batch simulation effort, were implemented and tested in a piloted-simulation study.

The results indicate that a recovery strategy based on flying a flight-path-angle schedule shows an improved performance over constant pitch attitude or acceleration-based recovery techniques. The performance difference between the three recovery techniques was less in the piloted simulation than was predicted by the batch simulation. The best recovery technique was initially counterintuitive to the pilots who participated in the study. Evidence was found to indicate that the techniques required for flight through the turbulent vortex of a microburst may differ from the techniques being developed using classical, nonturbulent microburst models.

## Introduction

Numerous air carrier accidents and incidents have resulted from inadvertent encounters with the atmospheric wind shear associated with microburst phenomena, in some cases resulting in a heavy loss of life. Fujita (ref. 1) defines a downburst as a strong downdraft that induces an outburst of damaging winds on or near the ground. He then classifies a microburst as a small downburst with its outburst damaging winds extending over a distance of 4 km (2.5 miles) or less. In general, an airplane penetrating a microburst will initially encounter an increasing head wind (which improves airplane performance), then a strong downdraft, and then a rapidly increasing tail wind. The downdraft and increasing tail wind effects may easily exceed the climb and acceleration capabilities of the airplane and thus cause an unavoidable loss of altitude and airspeed. These encounters have resulted from the fact that the ability to reliably predict or detect a microburst along an airplane flight path in an operational environment does not presently exist. The consequences of these encounters are exacerbated since the physics of microburst winds have only recently been understood in detail, and recovery during inadvertent airplane encounters may require techniques that are unique to microbursts and counterintuitive to flight crews.

The Federal Aviation Administration (FAA) and the National Aeronautics and Space Administration (NASA) are addressing the wind shear hazard through the Integrated Wind Shear Program. The goal of the plan is to reduce the hazard of low-level wind shear to aircraft through improved airborne and ground-based wind shear detection systems, crew alerting and flight guidance systems, and training and operating procedures. NASA is investigating the airborne aspects of the problem through hazard characterization, sensor technology, and flight management systems. This study addresses the recovery strategies that may be implemented by future flight management systems.

Previous research has investigated recovery strategies for maintaining a given flight path in the presence of strong wind shears (refs. 2 and 3). These studies have developed control laws to permit the airplane to track a predefined path, such as the glide slope of an instrument landing system. These control laws are not practical if the shear is severe. With currently available sensors, the severity of a shear cannot be known until the airplane has successfully flown through it. Other research (ref. 4) has shown the performance available from an airplane following an optimal trajectory that is based on full knowledge of a simplified microburst flow field. In that study the emphasis was on escape from inadvertent microburst encounters, and the trajectory was a result of the optimization procedure, not an assumed goal. Later research by the same authors investigated wind shear

recovery performance when only local wind knowledge was available (ref. 5), and they considered the maneuvering required of the pilot (ref. 6). Neither of these efforts, however, tested the proposed control laws in a piloted environment.

Additional research (ref. 7) was performed by NASA to develop recovery procedures that will produce "near optimal" recovery trajectories when the wind field ahead of the airplane is not known. That effort, which used analytical and batch simulation techniques to investigate recovery from microbursts encountered just after takeoff, showed that characteristics of optimal recoveries could be used to improve recovery performance significantly.

The characteristics of the recovery strategies that best utilized available airplane energy included an initial reduction in pitch attitude early in the encounter to reduce the climb rate, an increase in pitch (up to the stick-shaker angle of attack) late in the encounter, the smallest angle of climb necessary for obstacle clearance, and, if at a higher altitude than necessary, an intentional descent to reduce the airspeed deceleration. This technique minimized the time spent in the shear and kept the airplane flying above the stick-shaker airspeed for the greatest possible ground distance. Any unnecessary climb reduced the airplane speed excessively, increased the time spent in the shear, placed the airplane in a stronger downflow, and led to earlier stick-shaker activation. Minimum altitudes reached during recoveries were, in general, very sensitive to small variations in airplane state parameters or microburst strength and location. That study suggested that additional research needs to address the effects of turbulence and complex shear structures on the recovery strategies and piloting factors such as display options and the ability to follow the guidance.

This effort investigated the implementation, in a piloted-simulation environment, of three of the five recovery strategies developed in reference 7. This was done to develop both an understanding of how well theoretical predictions of wind shear recovery performance might be achieved in actual use and to gain insight into the piloting factors associated with recovery from wind shear encounters. The recovery guidance was presented on a conventional flight-director instrument in a generic, transport-category cockpit. Pilots performed manual takeoffs and encountered a microburst shortly after lift-off. Manual tracking of the recovery guidance was then performed. Data were collected on airplane state parameters, minimum altitudes reached during recoveries, root-mean-square tracking errors, and pilot comments.

## Abbreviations and Symbols

| | |
|---|---|
| ADI | attitude-director indicator |
| ANOVA | analysis of variance |
| AOA | angle of attack |
| $C_L$ | nondimensional lift coefficient |
| $C_{L,\max}$ | maximum lift coefficient |
| $C_{L,\mathrm{ss}}$ | lift coefficient needed for steady-state flight |
| $C_{L_\alpha}$ | change of lift coefficient with angle of attack, per degree |
| $D$ | total airplane drag, lbf |
| DFW | Dallas-Fort Worth |
| EPR | engine pressure ratio |
| $F$ | "$F$-factor" measure of wind shear impact on airplane flight-path-angle capability, rad |
| $g$ | gravitational acceleration ($1g \approx 32.174$ ft/sec$^2$), ft/sec$^2$ |
| $h$ | airplane altitude, ft |
| IRU | inertial reference unit |
| $K$ | gain in flight-path-angle control law |
| $KW$ | maximum horizontal wind, ft/sec |
| $L$ | total airplane lift, lbf |
| PIO | pilot-induced oscillation |
| RMS | root mean square |
| $S$ | airplane wing area, ft$^2$ |
| s.d. | standard deviation |
| $T$ | total engine thrust, lbf |
| $V$ | airplane true airspeed, ft/sec |
| $V_g$ | airplane ground speed, ft/sec |
| $V_2$ | takeoff safety speed, for second-segment climb, knots |
| VLDS | Langley Visual Landing Display System |
| VMS | Langley Visual Motion Simulator |
| VSI | vertical-speed indicator |
| $W$ | airplane weight, lb |
| $Wh$ | vertical wind speed, positive up, ft/sec |

| | |
|---|---|
| $Wx$ | horizontal wind speed, tail wind positive, ft/sec |
| $\Delta Wx$ | change in horizontal wind speed, knots |
| $X1$ | starting point of horizontal wind shear gradient, ft |
| $XL$ | width of horizontal wind shear gradient, ft |
| $x$ | horizontal distance across ground, ft |
| $\alpha$ | wing angle of attack, deg |
| $\alpha_c$ | angle-of-attack correction in flight-director algorithms, rad |
| $\gamma_a$ | flight-path angle with respect to air mass, rad |
| $\gamma_{a,c}$ | commanded air-mass flight-path angle, rad |
| $\gamma_{a,p}$ | potential flight-path angle with respect to air mass, rad |
| $\gamma_{i,c}$ | inertial, commanded flight-path angle, rad |
| $\gamma_{i,p}$ | inertial, potential flight-path angle, rad |
| $\theta$ | airplane pitch attitude, rad |
| $\theta_c$ | pitch-attitude command, deg |
| $\theta_{\text{fd}}$ | pitch-attitude bar drive for flight director, deg |
| $\lambda$ | gain in acceleration control law |
| $\rho$ | atmospheric density, slugs/ft$^3$ |

A dot above a symbol denotes a derivative with respect to time.

## Recovery Strategies

Three recovery strategies developed in reference 7 were selected for this effort. These were (1) pitch-hold, (2) acceleration, and (3) flight-path-angle strategies. The control laws used to implement the three recovery strategies are described in detail in appendix A. The control law gains used in this study were arrived at during simulation checkout sessions, based on best survivability.

The first strategy, pitch-hold, was selected as the baseline since it is the simplest and can be implemented easily on any airplane without adding sensors or performing equipment modification. Like the manual-recovery technique recommended by the FAA Wind Shear Training Aid (ref. 8), this recovery technique can be performed without adding wind shear recovery algorithms to existing flight-director systems. The pitch-hold strategy simply commanded the pilot to maintain a pitch attitude of 13° after encountering a wind shear.

The second recovery strategy chosen from reference 7 was the acceleration strategy. This strategy was selected since it could be retrofitted to airplanes that are not equipped with inertial reference units (IRU). This strategy traded off airspeed for climb-angle performance. The climb-angle performance lost to the wind shear can be described by the "$F$-factor" (introduced in ref. 9):

$$F = \frac{\dot{W}x}{g} - \frac{Wh}{V} \tag{1}$$

where $\dot{W}x$ is the rate of change of horizontal wind along the airplane flight path, $g$ is the gravitational acceleration, $Wh$ is the vertical wind speed, and $V$ is the airplane true airspeed. An increasing tail wind or decreasing head wind produces a positive $\dot{W}x$. An updraft produces a positive $Wh$. Data from the microburst models were used directly to determine $F$ without modeling airplane sensor or filter errors. A positive $F$-value of about 0.15 effectively cancels the climb capability of most transport-category airplanes. The acceleration control law was governed by the equation

$$\frac{\dot{V}}{g} + \lambda F = 0 \tag{2}$$

where $\lambda$ is a gain. In this study, airspeed rate was controlled solely by pitch changes since throttle control was saturated. In a performance-decreasing shear, a gain of 0 would produce a constant airspeed flight path that would pitch the airplane down and fail to use available climb performance. A gain of 1 would produce a constant ground speed flight path that would pitch the airplane up and rapidly use up the available kinetic energy. The gain in the acceleration law was set at 0.2 for this study.

Although the acceleration strategy could be implemented in numerous ways, the simplest method in this effort was to calculate the flight-path angle required to produce the desired airspeed rate. This flight-path angle was limited in descent to an angle of −2.9°. If a climb was required to produce the commanded airspeed rate, the climb angle was limited to an angle of 5.7° when airspeed was below 180 knots, and to the potential climb angle when airspeed was

above 180 knots. A climb may be required to produce the commanded airspeed rate in weak shears, in the sudden updrafts associated with vortex rings, or after exiting a shear. Potential climb angle is defined as the instantaneous climb angle that can be sustained with zero airspeed rate, given the airplane performance and the performance reduction due to the wind shear. Pneumatic total-energy sensor concepts (ref. 10) could be used to estimate the wind shear magnitude and command an airspeed rate.

Finally, the enhanced flight-path-angle strategy was selected from reference 7, and it will be referred to in this paper simply as the "flight-path-angle strategy." This recovery strategy was chosen since it provided the best overall results in that effort and is fundamentally different from the other strategies in that it manages airplane trajectory rather than state variables such as attitude or airspeed.

The flight-path-angle strategy guided the pilot along a flight-path angle that was a function of airplane altitude and wind shear strength. Below a 100-ft altitude, a positive inertial flight-path angle was targeted. This flight-path angle varied linearly from 1.72° at the surface to 0° at an altitude of 100 ft. Above 130 ft, the targeted flight-path angle was determined by multiplying the inertial, potential flight-path angle, which will by definition be negative in a severe shear, by a gain. This gain was set at 0.75 for the data runs. A commanded descent was the result. Between altitudes of 100 and 130 ft, the negative flight-path angle was linearly reduced from −1.72° at 130 ft to 0° at 100 ft. Negative flight-path angles were targeted only when the inertial, potential flight-path angle was negative. When the potential flight-path angle was positive, it was used as the target climb angle, regardless of airplane altitude. The flight-path-angle target was further limited in descent to an angle of −2.9°. In climb, the flight-path-angle target was limited to an angle of 5.7° when airspeed was below 180 knots, and to the actual, potential climb angle when airspeed was above 180 knots. This was the same flight-path-angle limiter used for the acceleration strategy. The calculated inertial flight-path-angle target was then used to calculate the pitch command that was displayed to the pilot.

The recovery strategies were presented to the pilot in the form of a pitch command on a conventional flight-director instrument. A pitch-command limiter was applied to the output of each control law to avoid commanding pitch attitudes that would cause the stick-shaker angle of attack to be exceeded. This limit was the sum of the stick-shaker angle of attack (15° with flaps set at 5°) and the air-mass relative flight-path angle. The rate of change of the stick-shaker pitch limit was limited to 3 deg/sec to dampen the response to the vertical wind gusts that would be experienced. In practice, the angle of attack would reach 15°, but the flight director would lower the commanded pitch to prevent an angle-of-attack increase. The rate of change of the final pitch command was also limited to 3 deg/sec for each control law.

## Microburst Models

Two microburst models (A and B) were utilized in the real-time simulation. Shear A was an analytical model based on an axisymmetric flow of an irrotational, inviscid fluid against a flat plate. This model was developed in reference 7 and is summarized here. Shear A is illustrated in figure 1. Horizontal winds were a function of the airplane position along the runway axis, and vertical winds were a function of altitude above the ground. Prior to reaching the microburst, the airplane experienced a steady head wind. While in the microburst, the horizontal wind varied linearly from the head wind to a tail wind of the same magnitude over a ground distance of 5000 ft. The equation for determining the horizontal wind while in the microburst is

$$Wx = \frac{2KW(x - X1)}{XL} - KW \tag{3}$$

where $Wx$ is the horizontal wind along the runway axis, $X1$ is the position of the start of the microburst, $x$ is the position of the airplane, $KW$ is the maximum value of the horizontal wind, and $XL$ is the length of the microburst (5000 ft). After microburst exit, a steady tail wind was encountered. The vertical wind is the same for all values of $x$, and is related to the horizontal wind by

$$Wh = -4KWh/XL \tag{4}$$

where $h$ is the altitude of the airplane. A limitation of the realism of this model is that the horizontal wind remains constant to infinity beyond the microburst width, and the vertical wind is the same for all horizontal positions. The model remains useful for this effort, however, since the shear is encountered very soon after takeoff, the airplane enters and exits the shear at low altitude, and the recovery is taking place near the center of the shear. Entry into the microburst was triggered when the airplane climbed through a predetermined altitude, usually 100 ft.

Three magnitudes of shear A were used. The weakest magnitude varied the horizontal wind component from a 45-knot head wind to a 45-knot tail wind for a total wind change of 90 knots. The intermediate level increased the outflows to 50 knots.

The strongest microburst had a 55-knot head wind changing to a 55-knot tail wind. The vertical wind speeds varied with the horizontal wind magnitudes according to equation (4). These magnitudes were established during the checkout sessions to produce a relatively survivable microburst in the weak case, a minimum recovery altitude of about 50 ft in the medium-strength microburst, and questionable survivability in the strong microburst. No lateral winds were generated. This microburst challenged only the performance capabilities of the airplane; there was no turbulence to complicate the tracking task or provide upsets to the airplane.

The second model, shear B, is illustrated in figure 2. This microburst challenged not only airplane performance but also introduced the control problems associated with the vertical and horizontal wind gusts that can be found in the vortex rings surrounding a microburst. This model is introduced in reference 8 as a takeoff-scenario training microburst. The vertical and lateral winds are based on the profile winds estimated from the Dallas-Fort Worth (DFW) wind shear accident (ref. 11), while a simple, linear, horizontal wind gradient is used. The winds at any point were a function only of the position of the airplane on the runway axis. The horizontal, vertical, and lateral winds were specified at given points along the runway axis. The winds vary linearly between the points specified. Like shear A, this microburst was initialized along the flight path at the beginning of each data run. When the airplane altitude first reached 100 ft, the microburst was repositioned so that the $x = 0$ point in the microburst model was at the present position of the airplane. The microburst then remained fixed spatially as the airplane flew through it. Prior to entering the microburst, all three component winds were zero.

The strength of shear B was adjusted by a gain that was applied to the magnitudes and rates of the three wind components. Figure 2 shows the base microburst with a gain of unity. The gains used in this study were 1.2 for a weak microburst, 1.25 for a medium strength microburst, and 1.3 for a strong microburst. This microburst model is not intended to provide a faithful reproduction of the DFW microburst, but only to include the characteristics of vortex-ring penetration. Shear B was used to study the effect of these characteristics on the performance achieved with the different recovery strategies.

The recovery control laws and a wind shear alert were triggered by a wind shear discrete signal (discrete). The discrete became "true" when the aircraft first entered the microburst at the preset altitude. The discrete remained true until three conditions were met. The conditions were (1) the airplane has flown out of the microburst, (2) the airplane has established a positive rate of climb, and (3) the airplane angle of attack has been reduced to less than 12°. In shear A, the airplane was considered to have flown out of the microburst at the point where the horizontal wind gradient goes to zero, 5000 ft after entry. In shear B the airplane was considered to have flown out of the microburst at the 8000-ft point on the microburst $x$-axis, where vertical and lateral winds are zero and the horizontal wind gradient is increasing airplane performance. The wind shear alert consisted of an audio tone and a red light located just above the ADI. The audio tone sounded for the first 5 sec of the encounter, and the red light remained illuminated as long as the wind shear discrete was true.

## Equipment

### Simulator Hardware

The Langley Visual Motion Simulator (VMS), which is a six-degree-of-freedom system, was utilized. The capabilities of this simulator are described in reference 12. This simulator provides a generic transport-airplane flight deck that is equipped with conventional electromechanical instrumentation, as shown in figure 3. The pilot was provided with an attitude-director indicator (ADI), airspeed indicator, turn and slip indicator, barometric altimeter, radar altimeter, vertical-speed indicator (VSI), heading indicator, and engine-pressure-ratio (EPR) instruments. Instrumentation errors, due to turbulence and the local pressure variations found in a microburst, were not modeled.

Flight-director commands were presented on the ADI by cross-pointer needles. A horizontally oriented needle moved vertically to give pitch-up/pitch-down commands, and a vertically oriented needle moved laterally to give roll-left/roll-right commands. The recovery guidance was presented to the pilot in the same format for all three control laws (appendix A). A pitch target was calculated to produce the required attitude, speed rate, or flight-path angle, and the flight-director pitch bar was positioned at that pitch value on the attitude indicator. When the airplane attitude matched the commanded pitch, the pitch bar was superimposed on the miniature airplane reference symbol. The roll channel of the flight director was active for each of the control laws. The roll bar was simply driven by bank angle so that the command was nulled whenever the wings were level. Full-scale deflection of the roll bar occurred at a bank angle of 40°. A fast/slow indicator in the ADI display was driven with angle of attack such that the

indicator was centered at the normal climb angle of attack, and the indicator reached the maximum slow index at the stick-shaker angle of attack. A red light centered just above the ADI and an audio tone were used to notify the pilot that the airplane had entered a microburst and that the recovery guidance was being displayed.

An out-the-window display of terrain was provided on the cockpit forward windows. This visual display was driven by a terrain model board referred to as the Visual Landing Display System (VLDS). The VLDS permitted the execution of visual takeoffs from a runway and provided visual attitude and altitude cues during the wind shear penetration. No visual meteorological cues or effects were shown. Audio cues for landing-gear retraction, wind noise, and engine noise were also provided.

Pilot control input was through a wheel and control column hydraulically loaded in pitch and roll, hydraulically loaded rudder pedals, and independent throttle levers. A stick shaker was implemented on the control column. Stick-shaker activation caused the control-column loader to produce a 9-cps, 0.10-in. oscillation of the column position. Landing gear and wing flap controls were also provided.

### Simulator Software

The simulator was driven with a full nonlinear math model of a Boeing 737-100 airplane with Pratt & Whitney JT8D-7 engines. The model included lift and drag coefficient data to an angle of attack of 24° and the effects on those coefficients of pitch rate, control deflection, and ground effect. In the event that angle of attack exceeded 24°, the software used the 24° value for lift and drag coefficients. The lift loss and drag increase due to roll-control spoiler deflection were modeled. Variations in aileron and elevator control forces with airspeed and trim position were fed back to the pilot. A landing-gear model permitted a takeoff ground roll and lift-off. This math model has been used at the Langley Research Center for numerous piloted simulations (ref. 13).

The airplane was configured for a gross takeoff weight of 100 000 lb at a center-of-gravity location of 20-percent mean aerodynamic chord. Standard sea level temperature and air density were selected. The corresponding limiting takeoff engine EPR of 1.95 produced a total thrust of about 24 000 lb at the rotational speed of 138 knots. The engines could be overboosted at that speed to a total maximum thrust of about 28 800 lb.

## Data

The data runs began with the airplane on the runway at a ground speed of zero. Data collection began during the takeoff roll when the airplane airspeed exceeded 120 knots and continued to the end of the run. Since the target rotational speed was 138 knots, data collection always began prior to lift-off. The wind shear was encountered after lift-off, and the run was terminated when the airplane successfully recovered from the shear or when the airplane crashed. The following variables were recorded at four samples per second: time, runway axis position of airplane, altitude, altitude rate, airspeed, airspeed rate, angle of attack, rate of change of angle of attack, pitch, pitch rate, pitch-attitude flight technical error (pitch error), total engine thrust, inertial flight-path angle, inertial potential flight-path angle, total energy rate, horizontal wind speed ($Wx$), rate of change of $Wx$, vertical wind speed ($Wh$), wind shear alert discrete, control surface deflection (elevator, ailerons, and rudder), and landing-gear position. The pitch-attitude flight technical error is defined as the difference between the pitch attitude commanded by the flight director and the actual airplane pitch attitude.

In addition to the raw data, root-mean-square (RMS) values of pitch error, pitch rate, and angle-of-attack rate were computed for only that portion of the run where the wind shear alert discrete was true. The takeoff roll and initial climb were therefore not included in the RMS data. The RMS values were computed as an indication of the ability of a pilot to follow flight-director guidance during a microburst encounter. A primary measure of the performance of a given recovery was recovery altitude, which was also determined from the raw data. Recovery altitude is defined as the lowest altitude encountered by the airplane, at the center-of-gravity location, after the airplane has begun to descend in the microburst. When the airplane crashed during a microburst encounter, the recovery altitude was defined to be zero. This lower bound on recovery altitude may produce some inaccuracies in the statistical analysis. In this study, the microburst was always entered with the airplane climbing, and the microbursts were sufficiently strong that a descent was produced in every run.

## Experiment Design and Procedure

The factors of primary interest in the experiment were variations in recovery strategy, microburst type, and microburst strength. It was desirable to detect any differences in the performance of the three strategies tested and how those performances might interact with variations in microburst type and strength. Seven combinations of shear type, strength, and

location were used. Shear A was flown with three magnitudes of total horizontal wind change (90 knots, 100 knots, and 110 knots) that were all entered at an altitude of 100 ft. Shear A was also flown with a horizontal wind change of 90 knots and with shear entry occurring at an altitude of 20 ft. The purpose of this scenario was to prevent the pilot from knowing that the microburst would always begin at 100 ft, and also to look at the performance of the strategies in encounters at very low altitudes. Shear B was flown with three gains (1.20, 1.25, and 1.30), all entered at an altitude of 100 ft. The seven microbursts were combined with the three recovery strategies to produce a 21-cell matrix. Three research test pilots participated in the study. Each pilot flew four runs in each cell for a total of 12 repetitions per cell. A total of 84 data runs was flown by each pilot for a complete total of 252 data runs. To reduce pilot fatigue, each pilot's data runs were distributed over at least 3 days. The order of the data runs for each pilot is shown in table 1. The runs were grouped into sets, where the strategy remained fixed within a set but the microburst type was randomized. This enabled the pilot to know which strategy would be in use for each run, but it prevented the pilot from knowing which microburst would be encountered.

During discussion of the results, the wind shear types will be designated as follows: The wind shears of type A that are entered at 100 ft will be labeled "A90," "A100," and "A110." The number in each case describes the change, in knots, of horizontal wind. The wind shear of type A entered at 20 ft will be labeled "ALOW." The wind shears of type B will be labeled "B1.2," "B1.25," and "B1.3." The number in each case describes the gain on the baseline wind magnitudes.

Prior to the start of the tests, each pilot was given a thorough briefing on the airplane type and related performance parameters; and a series of training runs were made with each of the strategies and microburst types. The pilots were instructed that takeoff would be made with the flight director commanding a normal-climb pitch attitude of 16°, and that the recovery guidance would automatically be selected at wind shear entry. The pilot was instructed to ask for landing-gear retraction at a normal height, but not to change the airplane configuration during the microburst encounter. The wing flaps were set at 5° for all takeoffs and remained at that setting. The function of each of the three recovery strategies was explained. Instructions were given to follow the recovery commands unless a higher pitch attitude became necessary to prevent ground contact or settling below the lowest altitude that the pilot was willing to accept. The pilots were advised, however, that since the flight-path-angle guidance was a function of altitude, it should not be necessary to increase pitch above the commanded value when using that strategy. The pilots were also advised of the stick-shaker angle-of-attack limiting in the flight-director algorithms and of the operation of the fast/slow indicator on the ADI as an angle-of-attack instrument.

## Results and Discussion

### Statistics

The parameters of primary interest for statistical analysis were recovery-altitude and pitch-attitude flight technical errors. Recovery altitude was examined as a measure of the performance of the recovery. The RMS pitch-attitude flight technical error was examined as an indication of the ability of a pilot to follow the guidance during a microburst encounter. Flight technical error can be generated both by difficulties in capturing the commanded pitch and by intentional deviations from the commanded pitch to avoid ground contact. The recovery altitude for each run is shown in table 2. The RMS of pitch-attitude flight technical error for each run is shown in table 3. The data are presented in the same run order as the data in table 2, so the RMS pitch error can be compared with the recovery altitude for each run. The mean and standard deviation of the recovery altitude for combinations of strategy and shear are presented in table 4 and in figure 4. The mean and standard deviation of the RMS pitch error for combinations of strategy and shear are shown in table 5. The data for only the high-altitude (100-ft) microburst encounters were used in the statistical analysis.

Analysis of variance (ANOVA) techniques were used on the data in table 2 to test the significance of the differences in recovery altitudes. The pitch-hold, acceleration, and flight-path-angle strategies produced average recovery altitudes of 79.8, 82.2, and 86.9 ft, respectively. A two-factor ANOVA was performed with factors strategies and shears, both by microburst strength and microburst type, and the results are shown in table 6. There is no interaction between the factors or any difference in performance between the recovery strategies indicated by the analysis. As would be expected, a difference in performance with different microbursts is indicated at a 0.01 level of significance. A two-factor ANOVA of the factors strategies and pilots was also performed and is shown in table 7. This test indicated no statistically significant interaction or differences in strategies. Differences in performance with different pilots are indicated at the 0.01 level of significance. Finally, a one-factor ANOVA was performed for each of the six shears with the recovery strategies as the factor.

The results are shown in table 8. No significant differences in the strategies were detected except in shear A110, in which differences were indicated at the 0.01 level of significance.

The RMS pitch-attitude flight technical errors were analyzed using a two-factor ANOVA, both for the factors strategies and shear and for the factors strategies and pilots. The ANOVA results are shown in tables 9 and 10. In both cases no interaction between the factors is indicated. Differences in the RMS flight-technical-error values with the factors strategies, shears, and pilots were all indicated at the 0.01 level of significance. It is apparent that guidance following is less precise in shear B, with the associated airplane disturbances, than in shear A. The overall, mean RMS pitch error was 2.45° for shear A and 3.87° for shear B. It is also apparent that the RMS error varies with the strategy in use, with the RMS error for the flight-path-angle strategy nearly 1° better than for the pitch-hold strategy. The RMS pitch-attitude flight technical error was 3.55°, 3.01°, and 2.63° for pitch-hold, acceleration, and flight-path-angle strategies, respectively.

The statistical analysis shows that there is no significant difference in the average recovery altitudes achieved with the three recovery strategies. Also apparent from the statistics is the fact that the differences in recovery altitude due to changes in microburst strength are much larger than the differences due to varying the recovery strategy. This is not surprising considering the sensitivity of recovery altitude to small changes in microburst strength, as described in reference 7. The analysis also shows that statistically significant differences in pilot tracking performance do exist between the different strategies and the different shear models.

## Comparison of Results With Batch Simulation Predictions

Although the average recovery altitudes of the three recovery strategies were statistically the same, further analysis and a comparison of the strategies reveal factors of interest for future recovery-strategy development. A comparison was made of the recovery performance results in the piloted simulation with performance predictions made using the batch simulation technique described in reference 7. The comparison parameter was recovery altitude, and the comparison was made for only shear A. This microburst was chosen since it is the nonturbulent shear, and the point-mass batch simulation program could not be expected to predict the response of the airplane or pilot to turbulent disturbances. To make the comparisons, batch simulations were conducted using initial conditions that closely approximated the state of the airplane as it entered the wind shear in the piloted runs. The initial conditions were a pitch attitude of 16°, an airspeed of 160 knots, and an altitude of 100 ft. The engine thrust of the airplane was fixed at the maximum overboost value of 28 800 lb. These initial conditions provided a slight performance benefit to the batch simulation airplane since the engines were already at maximum thrust upon entering the microburst, whereas a delay was associated with the thrust increase in the real-time simulation.

The control parameter of each recovery strategy was varied in the batch runs to attempt to encompass the results of the real-time runs. In the pitch recovery strategy, the target-recovery pitch attitude was varied from 10° to 16° in 1° increments. In the acceleration recovery strategy, the acceleration gain $\lambda$ was varied from 0.1 to 0.4 in increments of 0.1. In the flight-path-angle recovery strategy, the flight-path gain was varied from 0.65 to 0.85 in increments of 0.1.

Table 11 shows the numerical results of the batch runs along with the average recovery altitudes of the corresponding real-time runs. Figure 5 shows a graphic comparison between corresponding batch and real-time runs for each recovery strategy. For any given recovery strategy, it can be seen that the performance of the piloted simulation is generally less than that of the batch simulation. Recovery altitude with the pitch strategy was 36 to 57 ft less in the real-time simulation, but the trend toward reduced recovery altitude with increased microburst strength was similar in both simulations. Recovery altitude with the acceleration strategy agreed well between the two simulations, with the largest difference being 22 ft. The slope of the lines on figure 5, between shear A90 and shear A100, indicates the possibility that the acceleration strategy may be more sensitive to increases in microburst strength in the real-time simulation than in the batch simulation. It would not be possible for this trend to continue beyond shear A100 in this experiment since the recovery altitude cannot go below zero in shear A110. Recovery altitude with the flight-path-angle strategy varied greatly between the two simulations. In the batch simulation, the recovery altitude showed almost no sensitivity to changes in microburst strength and was between 100 and 104 ft. In the piloted simulation, the average recovery altitude showed the same type of sensitivity to microburst strength as the other strategies and varied from 114 to 29 ft.

The poor correlation between the batch results and the average real-time results could be due to the error present in piloted tracking of flight guidance, the high sensitivity of recovery performance to slight

variations in airplane state parameters or microburst strength and location, and the slightly lower performance of the real-time simulation in the microbursts tested. It was common during piloted data runs for the airplane to be climbing at a pitch greater than the nominal 16° at microburst entry, for a pilot to be slow in following the initial pitch-down command or to slightly lead or lag other pitch-change commands, or for the airplane to maintain an angle of attack beyond the stick-shaker limit.

The resulting flight technical error, combined with other differences in the airplane and microburst models in the two simulations, caused the real-time airplane to have slightly less performance in wind shear than the batch simulation. This put the real-time simulation in a situation where the stick-shaker angle of attack was usually encountered earlier than it is encountered with the batch simulation. The earlier stick-shaker activation caused small increases in microburst strength to result in large reductions in recovery altitude. In the real-time simulation, if the stick shaker was encountered with more than 5 sec of wind shear remaining, the airplane crashed. In the batch runs, the reason for constant recovery altitudes with varying microburst strength with the flight-path-angle strategy is that the stick-shaker angle of attack was not encountered in the two weakest microbursts and was encountered less than 1 sec from exiting the strongest microburst.

In examining the data in table 11, it can be seen that small changes in the control parameter generally caused large changes in the recovery altitudes for the pitch and acceleration strategies. For example, in shear A90 with the pitch recovery strategy, a target pitch of 11° produced a recovery altitude of 110 ft, whereas a target pitch of 15° produced a recovery at 212 ft. This may partially account for the large variations in recovery altitude seen in the piloted simulations for any given combination of microburst strength and strategy. In the real-time data cell for the acceleration strategy and shear B1.25, for example, one pilot crashed on one run and had a recovery altitude of 273 ft on another run.

The pilots in the real-time simulation were capable of achieving basically the same performance with the flight-path-angle strategy as was achieved in the batch simulation, as indicated by the data from runs 51 and 69 by pilot 1. Both runs used the most severe level of shear A, and no excess energy was present at shear entry. This result indicates that when the run is properly flown, the performance achieved in the real-time simulation can closely approximate the batch simulation predictions, and that the large discrepancies between the batch and real-time results are due to piloting factors.

Based on the results of this comparison between the batch and real-time simulation results, it appears that the batch simulations are useful for developing recovery concepts but they are limited in predicting which concept will do best in a piloted environment. The batch simulations indicated a strong sensitivity to variations in microburst strength and to changes in control law gains. This sensitivity was observed in the piloted simulations. The large performance increase predicted by the batch runs for the flight-path-angle strategy, however, was not realized in the piloted simulation because of piloting factors that generally caused variations in the flight path and earlier stick-shaker activation.

### Pilot Comments and Questionnaire Responses

In an effort to determine pilot acceptance of the wind shear recovery strategies and to gain insight into the piloting factors associated with manual flight through the shear, written questionnaires were given to the pilots during the sessions and general comments were encouraged. Appendix B provides a summary of the pilot responses to each of the questions on the written questionnaires and gives a further discussion of pilot comments.

The questionnaires and comments were examined for factors that might cause the pilot to be uncomfortable with the guidance or intentionally deviate from the commanded pitch. There was a reported insidious tendency of the pitch-hold control law to lead pilots into the ground. Neither the pitch-hold nor the acceleration control law utilized airplane altitude, and in some situations the flight-director bar would be centered after exiting a shear; yet the airplane would be descending at low altitude with the pitch attitude too low to arrest the descent promptly. Except for the flight-path-angle strategy, which attempted to limit the descent at 100 ft, the pilots were forced to scan raw data and decide when to deviate from the guidance. All three pilots indicated that when descending through an altitude of about 100 ft, they would deviate from the guidance if necessary to stop the descent.

This factor led to a strong pilot preference for the flight-path-angle strategy. The flight-path-angle control law utilized all pertinent parameters (such as altitude and the airplane energy situation) in the recovery, and hence did not require the pilot to process additional information. Control laws should consider all relevant parameters, such as energy rate, shear strength, and airplane altitude, to make the complex trade-offs that will be extremely difficult for a pilot to do during a microburst encounter.

The pilots made comments which directly compared the three recovery strategies. The pitch

strategy was considered the least useful of the group since the pilot had to disregard the commands during the later portions of the runs. The acceleration strategy, on the other hand, was initially reported to be a more natural, instinctive way to fly since no pitch-down at shear entry was commanded. Later, however, the pilots recognized the importance of an initial pitch reduction and made comments indicating that the acceleration strategy was too heavily biased toward gaining altitude. The flight-path-angle strategy seemed the most intelligent to the pilots, and positive comments were received about the preservation of kinetic energy and the commanded roundout at 100 ft.

The pilot comments raise training and design issues. Without an understanding of the trade-offs involved in a wind shear penetration, pilots may be reluctant to initially reduce the airplane pitch attitude upon entering a shear. It was more instinctive for the pilots to continue climbing. The comments, as well as the normal flying technique, also indicate that pilots will continue to scan other information during a shear penetration rather than rely solely on the flight director for guidance. The comments and run results suggest that when the flight-director guidance differs significantly from the instinctive flying technique, pilots may disregard or bias the guidance. It may therefore require an excessive and impractical level of training for air carrier crews to fully realize the benefits of control laws based on optimal trajectory techniques, or it may be necessary to provide control laws that are a compromise between an optimal technique and techniques that the pilots will readily accept.

### Plots of Airplane Trajectory and State Variables

Insights into the events occurring during a wind shear encounter can be gained from examination of plots of airplane altitude, angle of attack, pitch attitude, airspeed, pitch error, elevator deflection, and horizontal and vertical winds. All these parameters form the ordinate of the corresponding plot, and the distance traveled by the airplane along the runway axis forms the abscissa. The pitch error, which is defined as the difference between the pitch commanded by the flight director and the actual pitch attitude, represents the deviation of the flight-director pitch bar from the airplane symbol in the ADI. The data for each plot begin with the airplane on the runway at an airspeed of 120 knots and include the rotation and climb to the shear encounter. During the takeoff roll, the flight director commands a 16°-climb pitch attitude that is shown as a 16° pitch error on the pitch-error plots. The plots indicate the shear entry point and periods of flight where the stick shaker was activated.

A typical encounter with shear A with the pitch strategy is shown in figure 6. This run used the medium-strength shear with a total horizontal wind change of 100 knots. The plot of airplane altitude shows the takeoff, climb, and shear entry at a 100-ft altitude. The 13° pitch attitude used after shear entry resulted in a maximum height of about 300 ft, which was followed by a descent. The plot also shows the stick shaker activating at an altitude of about 150 ft and continuing during the pull-out maneuver. The recovery altitude was 77 ft. The pilot disregarded the pitch command and increased the angle of attack well above the stick-shaker limit during the pull-out. The pitch-attitude plot shows the takeoff rotation with an overshoot of about 5° past the 16° initial-climb pitch target. The pilot then rotated the airplane to the in-shear pitch target of 13° and attempted to maintain 13° until the pull-out was begun. Large pitch values were used in the final pull-out. The pitch-error plot shows the rotation command during the takeoff, the pitch-down command during the takeoff rotation overshoot, small oscillations about the commanded attitude during the shear, and the final deviation from the commanded attitude during the pull-out. It can be seen that this strategy attempts to conserve airspeed but that the pilot cannot blindly follow the guidance since it permits a descent and is open loop with respect to airplane altitude.

An encounter with the same shear, using the acceleration strategy, is shown in figure 7. The altitude plot shows a rapid climb and an early activation of the stick shaker, which continued to ground impact. The airspeed plot shows shear entry at a normal airspeed, then a rapid deceleration to an airspeed of about 107 knots. The $1g$ stall speed of the airplane in this configuration and weight is about 122 knots. The airspeed then increased during the descent to the ground, but insufficient altitude remained to arrest the descent. The pilot rotated to a very large angle of attack just prior to ground impact. The pitch-attitude plot shows shear entry very near the target pitch attitude, and a further increase in pitch to about 19° prior to stick-shaker activation. As a large negative flight-path angle developed, the pitch was lowered to less than 8° while the airplane remained at an excessive angle of attack. The pitch-error plot shows that the rapid climb was not entirely due to the guidance. During most of the climb, the pilot maintained a pitch attitude that was 1° to 5° above the commanded attitude. There was a trend, however, for the acceleration strategy to produce

trajectories that were higher than necessary with excessive airspeed loss.

A wind shear recovery in the same shear, using the flight-path-angle strategy, is shown in figure 8. The altitude plot shows the climb being stopped at a lower altitude than in the two previous examples, and then being followed by a straight-line descent. The final pull-out was then made with the stick shaker activated with a recovery altitude of 103 ft. The airspeed plot shows shear entry at a slightly lower than normal airspeed, a very low minimum speed, and the typical change in sign of airspeed rate upon exiting the shear. Excessive angle-of-attack values seen in the plots for the previous examples were not reached. The pitch-attitude plot shows the pitch being reduced to about 13° after shear entry and then remaining near this value until beginning the rotation to arrest the descent. This is the same pitch attitude commanded by the pitch strategy; but here the commanded pitch increased slowly as the airspeed dropped and increased further as the recovery altitude was reached. Examination of the pitch-error plot shows that after the initial pitch-down maneuver, the pilot maintained a pitch attitude very near the commanded value during the recovery. The pilot did allow an excessive pitch attitude to develop after the recovery. This situation often developed because of a tendency by the subject pilots to relax and stop flying the airplane after a recovery in anticipation of the simulator reset. In general, the flight-path-angle strategy produced a pushover from a climb to a controlled descent, a minimum pitch attitude of 10° to 13°, a slow increase in pitch attitude as airspeed decreased, and a commanded pull-up as the airplane approached an altitude of 100 ft.

The sensitivity of the recovery altitude to the initial shear-entry pitch attitude and to the aggressiveness of reducing the pitch attitude can be seen by comparing the pitch-strategy run previously described with the run shown in figure 9. Both runs were flown in the same shear by the same pilot. In the two runs, the pitch attitudes were similar and airspeed was nearly identical at wind shear entry. The altitude traces were very similar during most of the flight but a slightly lower entry attitude and a more aggressive pushover resulted in less airspeed loss in the run previously presented in figure 6. In this run the minimum airspeed was 119 knots, for a loss of 37 knots, and the recovery altitude was 77 ft. In the run of figure 9, the minimum airspeed was 113 knots, for a loss of 42 knots, and the airplane crashed. The difference in airspeed loss was 5 knots.

To appreciate the significance of this small airspeed difference to a recovery, consider the difference in $g$-loading possible at a given angle of attack. A 5-knot increase in speed at these airspeed values equates to an increase in available lift of about 10 percent. In the successful run of figure 6, the normal acceleration of the airplane varied from $0.99g$ to $1.04g$ as the pull-out was made. In the unsuccessful run of figure 9, the normal acceleration varied from $0.94g$ to $0.97g$ during the pull-out attempt. The pilot was able to obtain about 5 to 7 percent greater normal acceleration during the pull-out at the slightly higher airspeed.

A similar situation is seen in the runs shown in figure 10. Both runs were flown using the flight-path-angle strategy in the most severe magnitude of shear A where the total horizontal wind change is 110 knots. In the successful run, shown by the solid line, the shear was entered with a pitch attitude of 14.8° and the pitch attitude during the descent phase of the recovery varied around a value of 11°. In the unsuccessful run, shown by the dashed line, the shear was entered with a pitch attitude of 16.6° and the pitch attitude during the descent varied around 13°. In the successful run, the climb was arrested more aggressively and the airplane altitude during the initial descent was about 40 to 50 ft lower than in the unsuccessful run. Although the entry and minimum airspeeds were almost identical between the two runs, examination of the airspeed plot shows a different airspeed distribution. In the successful run, the airspeed rate was low early in the shear and increased rapidly late in the shear, as compared with the unsuccessful run. This produced a higher average airspeed in the shear (139 knots and 135 knots, respectively) and reduced the time flown in the shear (22 sec and 24 sec, respectively).

Additional factors were introduced in recoveries from shear B, which included the updraft and downdraft changes representative of flight through the vortex circulation ring at the base of a microburst. (See refs. 1 and 11.) In this vortex, pilot control of airplane pitch attitude became more difficult and less precise than in shear A. There is evidence in the plots that the pilot/airplane response to the vertical wind changes sometimes reinforced the effect of the wind change to produce large and sudden changes in airplane angle of attack and flight-path angle. In this particular shear model, airplane performance was limited largely by the vertical winds. The change in horizontal wind was only 68 knots over a horizontal distance of 5200 ft with the maximum gain used. This change compares with a 90-knot change in horizontal wind over a 5000-ft difference in the lowest gain of shear A.

A run in shear B with the shear gain set at 1.25 is shown in figure 11. The acceleration strategy was

used in this run. Examination of the altitude plot shows that the recovery was completed at a relatively high altitude and with three periods of stick-shaker activation. The airspeed plot shows that the airspeed remained within reasonable values during the encounter with a minimum value of 128 knots. Examination of the angle of attack, pitch attitude, and vertical wind plots shows that in the first downdraft, the pilot held a high pitch attitude of about 19° while the angle of attack dropped to only 6°. In the updraft that followed, the angle of attack exceeded the stick-shaker value, and the pitch was decreased. As the pitch was being lowered, the updraft decreased and became a downdraft, thus reducing the angle of attack faster than the pitch reduction alone would have. Next, the stick shaker deactivated and the pitch attitude was again increased. The downdraft again switched to an updraft, thus reactivating the stick shaker. The pitch attitude was once again reduced, just as the small updraft changed to a large downdraft. In this, the third downdraft, the vertical wind change combined with the decrease in pitch to produce an angle-of-attack change twice as large as the pitch-attitude change. The pitch was reduced from 18.5° to 12.5° while the angle of attack dropped from 18° to 6°. This occurred at low airspeed and produced the sudden change in flight-path angle seen on the altitude plot between the second and third periods of stick shaker. The pitch oscillations were about 180° out of phase with the flight-director commands. These pitch oscillations during the vortex penetration are typical of the other runs in this shear with all recovery strategies. The third downdraft frequently resulted in a sudden reduction in flight-path angle.

The sudden reductions in pitch cannot be attributed solely to pilot response to stick-shaker activation. A run in shear B where the stick shaker never activated is shown in figure 12. The lowest gain, 1.2, was used for the shear, and the pitch strategy was provided. The altitude plot shows the variations in flight-path angle during the vortex penetration. The pronounced decrease in flight-path angle at the 12 000-ft horizontal position corresponds to the third downdraft, as in the previous example. The airspeed plot shows that very high speeds were maintained. Airspeed never fell below 145 knots. The angle of attack and pitch plots, however, show oscillations that are similar to the previous example. Pitch varied approximately 5° each side of the commanded value of 13° during the vortex encounter. The elevator-position plot shows the pilot attempting to prevent the pitch excursions, but control inputs were out of phase with the changes in the vertical wind.

A final example of a vortex penetration is shown in figure 13. The highest gain of 1.3 was applied to the shear, and the flight-path-angle strategy was used. A reduction in flight-path angle accompanied the final two downdrafts, just after deactivation of the stick shaker. Despite adequate airspeed to maintain level flight, ground impact occurred after the final reduction in flight-path angle. The out-of-phase control inputs caused a large angle-of-attack reduction that combined with low airspeed to cause a sudden loss of lift and a reduction in flight-path angle.

From these plots, plots from other runs, and pilot comments, it appears that the vortex created a very high work load situation for the pilot. Precise attitude control was not possible. The period of the cycles in the vertical winds in this shear model was such that the pilot response to disturbances occasionally reinforced the effects of later disturbances. The final downdraft of the shear appears to have had a larger effect on flight path than the first two downdrafts. In the first downdraft, the airspeed was still high, the out-of-phase control inputs had not yet begun, and the intent of the control law was to reduce the flight-path angle. The effect of the downdraft was therefore masked. In the final downdraft, however, the airspeed was low, attitude control of the airplane was poor, and maintaining a reasonable flight-path angle was necessary. Once a loss of lift causes a reduction in flight-path angle, low airspeed limits the ability of the airplane to produce the increased lift needed to recover the flight-path angle.

The differences in the characteristics between flights through shear A and shear B have implications for recovery strategy development. In the classic microburst model, flight at the lowest practical altitude is favored to take advantage of the lower vertical winds and to preserve airspeed as long as possible. In shear A, unintentional descents occurred when the airspeed was reduced below a value that would sustain level flight. In shear B, unintentional descents occurred when a downdraft and low pitch attitude combined to produce a low angle of attack. This occurred both at low airspeeds and at airspeeds well above the 1$g$ stick-shaker speed. In a vortex ring, therefore, airplane control may be a greater concern than airspeed loss, and a higher altitude may be desirable to allow for sudden altitude losses that may occur during upsets. Automation or augmentation to reduce the airplane natural response to the vertical winds might increase the ability to recover from the vortex without large pitch-attitude excursions and the resulting flight-path deviations. It appears that shear B is best flown with higher pitch attitudes and airplane altitudes than are optimal for shear A. Further testing of strategies for the recovery from

vortex encounters will require a more sophisticated wind shear model than the one used in this analysis. As a minimum, the model must include vertical and horizontal winds that are a function of both horizontal and vertical airplane positions, both for the core of the microburst and for the surrounding vortex ring.

## Concluding Remarks

Real-time simulations of transport-airplane wind shear (microburst) encounters following takeoff were conducted to investigate the use of various recovery strategies in a piloted environment. Three recovery strategies were tested: (1) a simple pitch-attitude-hold strategy, (2) an acceleration strategy, and (3) a flight-path-angle strategy. The recovery strategies were implemented using a conventional electromechanical flight director.

The results indicate that the characteristics of a recovery strategy that maximizes available airplane performance in a takeoff wind shear encounter include an initial reduction in pitch attitude early in the encounter to reduce the climb rate, an increase in pitch (up to the stick-shaker angle of attack) late in the encounter, the smallest angle of climb necessary for obstacle clearance, and, if at a higher altitude than necessary, an intentional descent to reduce the airspeed deceleration. These characteristics minimize the time spent in the shear and keep the airplane flying above the $1g$ stick-shaker airspeed for the greatest possible ground distance.

The difference in performance between the three recovery strategies across all shears was not statistically significant, and recovery altitudes were generally less than those predicted by batch simulations. Results indicate that batch-simulation performance predictions could be achieved in the real-time simulation, and they suggest that piloting factors were responsible for the variability in performance. Considerations of pilot factors suggest that optimal trajectories will not be achieved if the required flight technique conflicts with instinctive flying technique. Further analysis and pilot comments indicate, however, that the flight-path-angle strategy is the most promising for future development.

The wind shear model that included the vortex-circulation effects introduced additional factors into the recoveries. The sudden updrafts and downdrafts in the vortex made precise control of pitch attitude impossible. Ground impact sometimes occurred when out-of-phase control inputs caused unintentional pitch reductions that occurred as the airplane entered a downdraft. In contrast, unintentional descents in the nonturbulent shear generally occurred when airspeed became inadequate to maintain level flight. The optimal recovery in a vortex penetration may therefore have different characteristics than an optimal recovery in a classical microburst model. More research is needed on the recovery from vortex-circulation encounters, and microburst models that include the vortex circulation are needed for that research.

NASA Langley Research Center
Hampton, VA 23665-5225
January 19, 1989

## Appendix A

## Real-Time Piloted-Simulation Flight-Director Control Laws

The flight-director control laws computed a target pitch to accomplish the objectives of each of the three recovery strategies. The flight-director pitch bar was then driven to that value on the pitch scale of the attitude indicator. The pilot determined the necessary control inputs to achieve the pitch target. For each of the control laws, the pitch-command rates were limited to 3 deg/sec, and the pitch command was limited to a value that would achieve the stick-shaker angle of attack. During the takeoff roll and initial climb, a pitch attitude of 16° was commanded. The recovery control law was invoked after entering a wind shear. The recovery control laws are depicted in figure 14.

The pitch-hold control law was the most simple. A fixed-pitch target of 13° was commanded after entering a shear. The other two control laws, acceleration and flight-path angle, calculated a target flight-path angle that was used to calculate the necessary pitch target. The pitch target was calculated from angle of attack and the commanded air-mass flight-path angle starting from

$$\theta = \gamma_a + \alpha \tag{A1}$$

Since, in general, the actual angle of attack will not be the value required for steady-state flight because of maneuvering, an additional term was added. The lift coefficient needed for flight at the commanded flight-path angle was calculated and compared with the actual lift coefficient to determine a correction to the actual angle of attack. This was done with the relationships

$$L = W \cos \gamma_a \tag{A2}$$

and

$$L = \frac{1}{2}\rho V^2 S C_L \tag{A3}$$

which give

$$C_{L,\mathrm{ss}} = \frac{2W \cos \gamma_a}{\rho V^2 S} \tag{A4}$$

Comparing the required lift coefficient to the actual lift coefficient and dividing by the lift-curve slope gives the angle-of-attack correction

$$\alpha_c = (C_L - C_{L,\mathrm{ss}}) \Big/ C_{L_\alpha} \tag{A5}$$

A fixed value of 0.106 for $C_{L_\alpha}$ was used, where the unit of degrees is used for angle of attack. The relationship between commanded flight-path angle and commanded pitch that was actually used was

$$\theta_c = \gamma_{a,c} + \alpha - \alpha_c \tag{A6}$$

The acceleration-based control law calculated an air-mass relative flight-path angle to produce the required airspeed deceleration. The relationship between airspeed rate and flight-path angle is

$$\gamma_{a,p} - \gamma_a = \frac{\dot{V}}{g} \tag{A7}$$

and the potential air-mass flight-path angle can be written as

$$\gamma_{a,p} = \frac{T - D}{W} - \frac{\dot{W}x}{g} \tag{A8}$$

Combining equations (A7) and (A8) gives the required flight-path angle for a given airspeed acceleration:

$$\gamma_a = \frac{T - D}{W} - \frac{\dot{W}x}{g} - \frac{\dot{V}}{g} \tag{A9}$$

The governing equation for the acceleration control law is

$$\frac{\dot{V}}{g} = -\lambda F \tag{A10}$$

where $F$ is the "$F$-factor":

$$F = \frac{\dot{W}x}{g} - \frac{Wh}{V_g} \tag{A11}$$

Combining equations (A9), (A10), and (A11) produces the commanded air-mass flight-path angle for the acceleration control law

$$\gamma_{a,c} = \frac{T - D}{W} + (\lambda - 1)\frac{\dot{W}x}{g} - \lambda\frac{Wh}{V_g} \tag{A12}$$

A value of 0.2 was used for $\lambda$ during the tests.

The flight-path-angle control law determined an inertial flight-path angle as a function of altitude and wind shear strength. The wind shear strength was included in the potential flight-path-angle equation:

$$\gamma_{i,p} = \left(\frac{T - D}{W} - \frac{\dot{W}x}{g}\right)\frac{V}{V_g} + \frac{Wh}{V_g} \tag{A13}$$

The first step in calculating the commanded flight-path angle was to consider the airplane altitude and

potential flight-path angle. (Altitude is expressed in feet and angles in radians.) Thus, if $h \leq 100$, then

$$\gamma_{i,c} = 0.03 - \frac{0.03h}{100} \tag{A14a}$$

if $100 < h \leq 130$, then

$$\gamma_{i,c} = \frac{-0.03(h - 100)}{30} \tag{A14b}$$

and if $h > 130$, then

$$\gamma_{i,c} = K\gamma_{i,p} \tag{A14c}$$

The gain $K$ was set at 0.75 during the tests. To ensure that the airplane climbed when the wind shear strength permitted, the result of equations (A14) was compared with the potential flight-path angle, and the larger value was used. Finally, the commanded flight-path angle was limited. The limit descent angle was 2.9°. The commanded climb angle was limited to 5.7° if the airspeed was less than or equal to 180 knots, and it was limited to the potential flight-path angle if the airspeed was greater than 180 knots. The result was a commanded inertial flight-path angle, which was converted to an air-mass flight-path angle using the relationship

$$\gamma_{a,c} = \gamma_{i,c}\frac{V_g}{V} - \frac{Wh}{V} \tag{A15}$$

The resulting air-mass flight-path-angle command from equation (A12) or (A15), depending on the recovery strategy in use, was input to equation (A6) to determine the pitch command. The rate of change of the pitch command was limited to 3 deg/sec, and then it was further limited by stick-shaker angle-of-attack consideration. The pitch limit for the stick shaker was simply the sum of the air-mass flight-path angle and the limiting angle of attack (15°). The rate of change of the pitch limit was also limited to 3 deg/sec to prevent sudden pitch-down commands in the presence of vertical wind gusts.

## Appendix B

## Summary of Pilot Questionnaire Responses and Comments

The pilots were given 1-page questionnaires between certain runs to evaluate the recovery strategy and display. The questionnaire for each recovery strategy was given after the first set of six runs with that strategy, and it was given again after all data runs had been completed by that pilot. The pilots were also encouraged to provide general comments during the study. In addition to the primary issues addressed in the text, comments were received from the pilots regarding their reaction to commanded pitch reductions and their assessment of the guidance display format.

The pitch and flight-path-angle recovery strategies called for a reduced pitch attitude upon shear entry. With respect to this initial pitch-down command, the pilots were initially surprised and reluctant to follow the command, especially when they had not yet observed an airspeed decrease or climb degradation. Early in the experiment, one pilot expressed a desire to maintain the initial-climb pitch and gain altitude until the airspeed had decayed, perhaps as low as $V_2$. By the end of his data runs, however, that pilot had made positive comments about the importance of aggressively lowering the nose to follow the guidance. Another pilot, with previous experience in wind shear recovery experiments, indicated that he was not having any problem with the initial pitch-down command. With respect to the intentional descent produced by the flight-path-angle strategy, comments indicated that an intentional descent, managed by an intelligent control law, is acceptable.

Regarding the display format, the pilots strongly believed that the lateral steering bar should not be used. The pilots indicated that this bar was very distracting in turbulence and that no help was needed from the flight director in leveling the wings. The angle-of-attack information that was presented on the fast/slow indicator, on the left side of the attitude-director indicator, was generally of no help to the pilots. Some comments indicated that the instrument was nice to have, but it was not obvious how to use it. Other comments indicated that the instrument was telling the obvious, that it was too active in turbulence, and that it would be very difficult to use it in controlling the airplane. One pilot indicated that it was sufficient for angle of attack to be included in the recovery control law. Additional information presentation desired by the pilots consisted of actual flight-path angle, radar altitude on rising runway symbology, angle of attack with a reference mark at the angle of attack for maximum lift, and a means of signaling the increase in airplane energy after exiting the shear. Some comments indicated, however, that the pilot was too busy to take in any additional information and that he would not have much time to process any information concerning the shear itself. In general, the pilots liked the automatic switching of the flight director from the normal climb mode to the recovery guidance mode. The pilots believed that this was desirable and reduced the number of pilot decisions required.

The following is a summary of specific answers and comments given to each question on the questionnaire. The author has provided comments in parentheses in the answers to explain which recovery strategy the answer was given for or to indicate at what stage of the pilot's run matrix the answer was given.

1. Is the automatic switching of the flight director from the climb target pitch to the wind shear recovery guidance acceptable? Desirable?

   PILOT 1:

   Reduced the decision process of the captain.

   Yes, to both.

   Feel like "aggressive" following is important. (This answer was given after all the pilot's runs.)

   PILOT 2:

   Yes, both.

   PILOT 3:

   Yes, desirable.

   Very smooth, desirable from the standpoint of being reasonably easy to follow (acceleration strategy).

Acceptable, not always desirable, may be wrong command.

Yes, because early intervention is desirable if necessary.

2. Is the presentation of the recovery guidance acceptable? Is the use of the ADI fast/slow bug as an AOA meter useful? Any suggestions for display improvements?

PILOT 1:

The specific pitch guidance seems to require too much pushover (pitch strategy).

Yes (the presentation).

Have not incorporated AOA into cross-check.

AOA raw data add nothing, assuming AOA is incorporated into guidance.

Possible application of meter to hold AOA for $C_{L,\max}$.

Pitch guidance is okay if using raw speed to detect increasing kinetic energy.

Could add something to indicate speed is increasing.
(The last two answers refer to the airspeed increase seen when the airplane exits the wind shear.)

PILOT 2:

Generally good in pitch.

Lateral steering not desirable.

Learned to use AOA bug, good in smooth shear.

Using airspeed, never looked at AOA bug. (This answer was given after all the pilot's runs.)

PILOT 3:

Yes, acceptable.

Fast/slow bug is useful as it gives AOA decay information on flight director, nice to know margin from stick shaker.

Fast/slow bug somewhat useful, but in very general way.

3. What additional information concerning the wind shear, the aircraft energy/altitude state, or the guidance would you like to see displayed?

PILOT 1:

Further information on the subsiding of the wind shear.

A kinetic energy meter to show increasing trends after losses.

Advisability of configuration change during some portion, for example, calling for approach flaps when descending through 100 ft.

PILOT 2:

I've got all I can use now.

Possibly radar altitude in runway symbology.

Not much time for shear analysis.

None, no time.

PILOT 3:

Nothing - I'm not aware of what additional information would help except for knowing how long the shear area is and how much longer I can expect to be in it or how much worse it will get.

4. Does following the guidance seem natural, or is there a desire to depart from the commanded pitch and fly your own pitch schedule?

PILOT 1:

Feel like I should hold the climb attitude (gain altitude) until first positive decrease in speed (until $V_2$). (This answer was given during the early runs and referred to the pitch strategy.)

Does not seem natural, led to two near-crashes. (This answer was given after all the pilot's runs and referred to the pitch strategy.)

Seems natural, instinctive, seems to minimize control-column input requirements. (This answer was given during the pilot's early runs and referred to the acceleration strategy.)

Seems natural, sort of, seems to lead to out-of-phase pilot inputs under turbulent conditions. (This answer was given after all the pilot's runs and referred to the acceleration strategy.)

Seems natural, no desire to depart except for last-ditch effort (flight-path-angle strategy).

PILOT 2:

Is function of guidance law and what you see out the window.

Will depart from guidance below 100 ft, out the window.

Only when the ground is rushing up to meet you, then pull.

Oscillatory initially in smooth shear, worked well in turbulent shear (acceleration strategy).

Seems natural, just not very good (acceleration strategy).

Best of the bunch in turbulence (flight-path-angle strategy).

Seems natural (flight-path-angle strategy).

PILOT 3:

Seems somewhat abrupt and arbitrary. Since I can't see outside without stretching and I tend to PIO (pilot-induced oscillation) in following the flight-director command, I would like to be able to see the outside world and use this feedback to fly the airplane more smoothly. (This answer was given during the pilot's early runs and referred to the pitch strategy.)

Guidance seems very natural. It seems "smart" and I don't tend to want to fly my own pitch except momentarily to perhaps soften crash impact. (This answer was given during the pilot's early runs and referred to the acceleration strategy.)

This seems to be a smarter system. I have faith in its judgment until I am shown a system that does better. (This answer was given during the pilot's early runs, but after the above comment, and referred to the flight-path-angle strategy.)

Not natural, too simplistic and obviously not always appropriate. There is a desire to use my own pitch, especially when sink rate is increasing and altitude approaches 125 ft descending. (This answer was given after all the pilot's runs and referred to the pitch strategy.)

Only when in extreme situation do I want to depart from guidance. (This answer was given after all the pilot's runs and referred to the acceleration strategy.)

This is the most natural guidance of the three systems. (This answer was given after all the pilot's runs and referred to the flight-path-angle strategy.)

5. Comment on your ability to track the guidance (smooth shear and turbulent shear).

PILOT 1:

Not able to track tightly.

Don't feel that it needs to be precision tracking.

Don't believe in fighting natural response of airplane, within bounds.

Okay until 100-ft altitude in smooth shear, out of phase in turbulent shear. (This answer was given after all the pilot's runs and referred to the acceleration strategy.)

Good, both smooth and turbulent. (This answer was given after all the pilot's runs and referred to the flight-path-angle strategy.)

PILOT 2:

Smooth shear OK.

Could not center pitch-steering bar in turbulent shear.

Better than pitch guidance, I think (acceleration strategy).

Best of the bunch in turbulence (flight-path-angle strategy).

Difficult but possible with learning.

Trackable with high gain from pilot (acceleration strategy).

Oscillatory with high gain from pilot (flight-path-angle strategy).

PILOT 3:

Relatively good, made harder by push forces needed to follow flight director. (This answer was given during the pilot's early runs and referred to the pitch strategy.)

Generally good in smooth shear. However, in rough shear, the bank angle puts the roll bar way off to one side and at the same time the nose pitches down. Then, distance of flight-director bar intersection from airplane symbol is distracting. (This answer was given during the pilot's early runs and referred to the acceleration strategy.)

Good in both cases, in rough shear a tendency to fly a slightly excessive pitch. (This answer was given during the pilot's early runs and referred to the flight-path-angle strategy.)

Pretty good, but some chasing in oscillatory manner and some pushing on wheel required, harder with turbulent air than with smooth. (This answer was given after all the pilot's runs and referred to the pitch and acceleration strategies.)

Pretty good except for strong DFW-like (Dallas-Fort Worth) disturbances. (This answer was given after all the pilot's runs and referred to the flight-path-angle strategy.)

6. Any suggestions for improvements to the guidance law?

PILOT 1:

Improvements needed for acceleration guidance. (This answer was given after all the pilot's runs.)

PILOT 2:

Should be aware of altitude (pitch strategy).

Might look at adding flight-path angle to display (flight-path-angle strategy).

A little damping of the pitch-command bar during pilot inputs (flight-path-angle strategy).

PILOT 3:

Make it smarter (pitch and acceleration strategy).

7. Is the initial pitch-down/intentional descent acceptable? (This question was asked only on the questionnaires for the acceleration and flight-path-angle strategies.)

PILOT 1:

Perceived reasonable, commanded level flight, that was good. (This answer was given during the pilot's early runs and referred to the flight-path-angle strategy.)

Yes.

PILOT 2:

Okay, yes.

Was not aware of initial pitch-down (acceleration strategy).

PILOT 3:

Yes, in one run some chasing of pitch bar occurred initially but soon damped out. (This answer was given during the pilot's early runs and referred to the acceleration strategy.)

Yes (flight-path-angle strategy).

Yes, more natural than pitch guidance. (This answer was given after all the pilot's runs and referred to the acceleration strategy.)

## References


1. Fujita, T. Theodore: *The Downburst—Microburst and Macroburst.* SMRP-RP-210, Univ. of Chicago, 1985. (Available from NTIS as PB85 148 880.)
2. Psiaki, Mark L.; and Stengel, Robert F.: Analysis of Aircraft Control Strategies for Microburst Encounter. AIAA-84-0238, Jan. 1984.
3. Psiaki, Mark L.; and Stengel, Robert F.: Optimal Flight Paths Through Microburst Wind Profiles. *J. Aircr.*, vol. 23, no. 8, Aug. 1986, pp. 629–635.
4. Miele, A.; Wang, T.; and Melvin, W. W.: *Optimal Flight Trajectories in the Presence of Windshear. Part 4, Numerical Results, Take-Off.* Aero-Astronaut. Rep. No. 194, Rice Univ., 1985.
5. Miele, A.; Wang, T.; and Melvin, W. W.: *Maximum Survival Capability of an Aircraft in a Severe Windshear.* Aero-Astronaut. Rep. No. 213, Rice Univ., 1986.
6. Miele, A.; Wang, T.; and Melvin, W. W.: *Gamma Guidance Schemes and Piloting Implications for Flight in a Windshear.* Aero-Astronaut. Rep. No. 212, Rice Univ., 1986.
7. Hinton, David A.: *Flight-Management Strategies for Escape From Microburst Encounters.* NASA TM-4057, 1988.
8. Boeing Co.: *Wind Shear Training Aid. Volume 1—Overview Pilot Guide, Training Program.* Contract DFTAO-1-86-C-00005, Feb. 1987. (Available from NTIS as PB88 127 196.)
9. Bracalente, E. M.; and Delnore, V. E., compilers: *Wind Shear Detection—Forward-Looking Sensor Technology.* NASA CP-10004, DOT/FAA/PS-87/2, 1987.
10. Ostroff, Aaron J.; Hueschen, Richard M.; Hellbaum, R. F.; Belcastro, Christine M.; and Creedon, J. F.: *Evaluation of a Total Energy-Rate Sensor on a Transport Airplane.* NASA TP-2212, 1983.
11. Fujita, T. Theodore: *DFW Microburst.* NASA CR-176794, 1986.
12. Ashworth, Billy R.; McKissick, Burnell T.; and Parrish, Russell V.: *Effects of Motion Base and g-Seat Cueing on Simulator Pilot Performance.* NASA TP-2247, 1984.
13. Bowles, Roland L.; and Frost, Walter, eds.: *Wind Shear/Turbulence Inputs to Flight Simulation and Systems Certification.* NASA CP-2474, 1987.

Table 1. Real-Time Simulation Data Runs

[The gain represents the horizontal wind change, in knots, for shear A and a multiplier on the wind components for shear B]

| Run | Shear | Gain | Encounter altitude, ft | Strategy |
|---|---|---|---|---|
| 1 | A | 90 | 100 | Pitch-hold |
| 2 | A | 90 | 100 | ↓ |
| 3 | A | 110 | 100 | ↓ |
| 4 | B | 1.20 | 100 | ↓ |
| 5 | B | 1.25 | 100 | ↓ |
| 6 | A | 90 | 20 | ↓ |
| 7 | A | 90 | 100 | Acceleration |
| 8 | A | 90 | 100 | ↓ |
| 9 | B | 1.20 | 100 | ↓ |
| 10 | A | 90 | 20 | ↓ |
| 11 | B | 1.25 | 100 | ↓ |
| 12 | A | 110 | 100 | ↓ |
| 13 | A | 90 | 100 | Flight path |
| 14 | A | 90 | 100 | ↓ |
| 15 | B | 1.20 | 100 | ↓ |
| 16 | B | 1.25 | 100 | ↓ |
| 17 | A | 90 | 20 | ↓ |
| 18 | A | 110 | 100 | ↓ |
| 19 | B | 1.25 | 100 | Pitch-hold |
| 20 | B | 1.25 | 100 | ↓ |
| 21 | A | 100 | 100 | ↓ |
| 22 | A | 100 | 100 | ↓ |
| 23 | A | 90 | 20 | ↓ |
| 24 | B | 1.30 | 100 | ↓ |
| 25 | A | 100 | 100 | Acceleration |
| 26 | A | 100 | 100 | ↓ |
| 27 | B | 1.25 | 100 | ↓ |
| 28 | B | 1.30 | 100 | ↓ |
| 29 | A | 90 | 20 | ↓ |
| 30 | B | 1.20 | 100 | ↓ |
| 31 | A | 100 | 100 | Flight path |
| 32 | A | 100 | 100 | ↓ |
| 33 | A | 110 | 100 | ↓ |
| 34 | B | 1.30 | 100 | ↓ |
| 35 | B | 1.25 | 100 | ↓ |
| 36 | B | 1.25 | 100 | ↓ |
| 37 | A | 110 | 100 | Pitch-hold |
| 38 | B | 1.20 | 100 | ↓ |
| 39 | A | 90 | 20 | ↓ |
| 40 | B | 1.30 | 100 | ↓ |
| 41 | A | 90 | 100 | ↓ |
| 42 | B | 1.30 | 100 | ↓ |

Table 1. Concluded

| Run | Shear | Gain | Encounter altitude, ft | Strategy |
|---|---|---|---|---|
| 43 | A | 90 | 20 | Acceleration |
| 44 | B | 1.25 | 100 | |
| 45 | B | 1.25 | 100 | |
| 46 | A | 110 | 100 | |
| 47 | A | 110 | 100 | |
| 48 | B | 1.30 | 100 | |
| 49 | A | 90 | 100 | Flight path |
| 50 | A | 100 | 100 | |
| 51 | A | 110 | 100 | |
| 52 | B | 1.20 | 100 | |
| 53 | A | 90 | 20 | |
| 54 | B | 1.30 | 100 | |
| 55 | A | 100 | 100 | Pitch-hold |
| 56 | A | 100 | 100 | |
| 57 | B | 1.20 | 100 | |
| 58 | B | 1.20 | 100 | |
| 59 | A | 110 | 100 | |
| 60 | A | 110 | 100 | |
| 61 | B | 1.20 | 100 | Acceleration |
| 62 | B | 1.20 | 100 | |
| 63 | A | 90 | 100 | |
| 64 | A | 100 | 100 | |
| 65 | B | 1.30 | 100 | |
| 66 | B | 1.30 | 100 | |
| 67 | A | 90 | 100 | Flight path |
| 68 | B | 1.20 | 100 | |
| 69 | A | 110 | 100 | |
| 70 | B | 1.30 | 100 | |
| 71 | A | 100 | 100 | |
| 72 | A | 90 | 20 | |
| 73 | A | 90 | 100 | Pitch-hold |
| 74 | B | 1.25 | 100 | |
| 75 | B | 1.30 | 100 | |
| 76 | A | 90 | 20 | |
| 77 | A | 90 | 100 | Acceleration |
| 78 | A | 110 | 100 | |
| 79 | A | 90 | 20 | |
| 80 | A | 100 | 100 | |
| 81 | B | 1.20 | 100 | Flight path |
| 82 | B | 1.30 | 100 | |
| 83 | A | 90 | 20 | |
| 84 | B | 1.25 | 100 | |

Table 2. Recovery Altitude for Each Real-Time Run

| Run | Recovery altitude, ft, for— | | |
|---|---|---|---|
| | Pilot 1 | Pilot 2 | Pilot 3 |
| 1 | 153.2 | 131.8 | 149.2 |
| 2 | 121.8 | 109.7 | 122.9 |
| 3 | 0 | 0 | 0 |
| 4 | 206.2 | 73.9 | 140.1 |
| 5 | 83.9 | 44.9 | 51.5 |
| 6 | 118.8 | 99.5 | 104.2 |
| 7 | 130.4 | 163.0 | 144.3 |
| 8 | 203.4 | 31.9 | 138.9 |
| 9 | 237.6 | 177.1 | 56.6 |
| 10 | 137.7 | 170.3 | 144.7 |
| 11 | 148.6 | 0 | 0 |
| 12 | 0 | 0 | 0 |
| 13 | 167.5 | 89.6 | 99.4 |
| 14 | 141.4 | 89.8 | 92.2 |
| 15 | 177.1 | 117.6 | 86.4 |
| 16 | 128.1 | 0 | 32.3 |
| 17 | 138.7 | 71.5 | 87.5 |
| 18 | 0 | 0 | 0 |
| 19 | 191.6 | 22.7 | 44.5 |
| 20 | 154.2 | 51.6 | 80.1 |
| 21 | 0 | 0 | 38.8 |
| 22 | 77.1 | 51.4 | 0 |
| 23 | 91.2 | 77.0 | 0 |
| 24 | 93.4 | 0 | 0 |
| 25 | 0 | 85.3 | 71.0 |
| 26 | 0 | 0 | 0 |
| 27 | 0 | 182.8 | 0 |
| 28 | 0 | 133.2 | 0 |
| 29 | 0 | 169.9 | 0 |
| 30 | 205.0 | 223.9 | 48.4 |
| 31 | 77.5 | 78.4 | 49.2 |
| 32 | 103.1 | 106.8 | 0 |
| 33 | 0 | 45.4 | 0 |
| 34 | 0 | 161.3 | 0 |
| 35 | 102.3 | 142.4 | 90.5 |
| 36 | 58.4 | 192.6 | 69.9 |
| 37 | 0 | 25.1 | 0 |
| 38 | 196.4 | 134.7 | 73.4 |
| 39 | 107.0 | 132.6 | 118.2 |
| 40 | 177.0 | 35.9 | 0 |
| 41 | 168.9 | 147.2 | 121.8 |
| 42 | 138.2 | 94.5 | 36.5 |

Table 2. Concluded

| Run | Recovery altitude, ft, for— | | |
|---|---|---|---|
| | Pilot 1 | Pilot 2 | Pilot 3 |
| 43 | 78.3 | 191.9 | 107.6 |
| 44 | 273.6 | 121.0 | 0 |
| 45 | 113.3 | 193.7 | 0 |
| 46 | 0 | 0 | 0 |
| 47 | 0 | 0 | 0 |
| 48 | 57.5 | 225.8 | 0 |
| 49 | 89.5 | 86.5 | 132.7 |
| 50 | 114.7 | 89.8 | 91.9 |
| 51 | 91.1 | 52.8 | 41.1 |
| 52 | 197.1 | 179.3 | 117.4 |
| 53 | 110.1 | 88.9 | 97.7 |
| 54 | 0 | 0 | 0 |
| 55 | 84.8 | 84.7 | 102.3 |
| 56 | 107.2 | 65.7 | 74.3 |
| 57 | 152.3 | 108.6 | 65.5 |
| 58 | 111.9 | 154.5 | 89.2 |
| 59 | 0 | 22.6 | 0 |
| 60 | 0 | 0 | 0 |
| 61 | 161.5 | 248.7 | 150.4 |
| 62 | 242.2 | 248.8 | 0 |
| 63 | 215.9 | 194.9 | 12.4 |
| 64 | 71.3 | 86.7 | 0 |
| 65 | 79.7 | 37.9 | 0 |
| 66 | 87.1 | 0 | 0 |
| 67 | 112.7 | 158.1 | 109.7 |
| 68 | 160.9 | 164.8 | 59.9 |
| 69 | 96.0 | 24.3 | 0 |
| 70 | 90.8 | 0 | 0 |
| 71 | 94.4 | 70.6 | 0 |
| 72 | 106.3 | 116.0 | 96.4 |
| 73 | 127.9 | 112.2 | 127.5 |
| 74 | 52.8 | 151.3 | 0 |
| 75 | 43.2 | 82.1 | 0 |
| 76 | 108.7 | 127.2 | 152.0 |
| 77 | 226.1 | 0 | 158.8 |
| 78 | 0 | 0 | 0 |
| 79 | 82.4 | 126.2 | 0 |
| 80 | 109.6 | 0 | 0 |
| 81 | 167.9 | 175.1 | 189.5 |
| 82 | 76.1 | 100.9 | 0 |
| 83 | 100.0 | 94.9 | 125.5 |
| 84 | 158.2 | 215.0 | 55.7 |

Table 3. RMS Pitch-Attitude Flight Technical Error for Each Real-Time Run

| Run | RMS pitch-attitude error, deg, for— | | |
|---|---|---|---|
| | Pilot 1 | Pilot 2 | Pilot 3 |
| 1 | 1.530 | 2.176 | 1.683 |
| 2 | 2.238 | 1.880 | 1.969 |
| 3 | 2.460 | 1.630 | 1.985 |
| 4 | 4.092 | 4.475 | 3.050 |
| 5 | 4.653 | 4.543 | 3.685 |
| 6 | 2.317 | 1.242 | 1.392 |
| 7 | 1.864 | 1.933 | 2.296 |
| 8 | 1.474 | 2.060 | 1.360 |
| 9 | 3.225 | 3.673 | 3.812 |
| 10 | 2.086 | 1.433 | 1.844 |
| 11 | 3.809 | 4.159 | 3.290 |
| 12 | 2.886 | 3.127 | 2.075 |
| 13 | 1.856 | 1.887 | 1.498 |
| 14 | 1.977 | 2.268 | 1.536 |
| 15 | 4.389 | 2.922 | 2.772 |
| 16 | 2.945 | 3.851 | 2.895 |
| 17 | 1.989 | 1.986 | 1.742 |
| 18 | 2.332 | 1.897 | 1.527 |
| 19 | 5.591 | 6.821 | 5.629 |
| 20 | 4.265 | 4.500 | 6.131 |
| 21 | 4.459 | 2.201 | 4.189 |
| 22 | 5.303 | 1.987 | 4.953 |
| 23 | 6.654 | 1.709 | 6.041 |
| 24 | 4.071 | 2.245 | 3.275 |
| 25 | 2.719 | 2.421 | 1.867 |
| 26 | 3.270 | 3.401 | 1.763 |
| 27 | 5.465 | 3.593 | 7.312 |
| 28 | 5.223 | 2.832 | 3.012 |
| 29 | 4.950 | 1.595 | 2.417 |
| 30 | 3.234 | 2.782 | 4.228 |
| 31 | 2.362 | 1.533 | 3.229 |
| 32 | 2.922 | 2.266 | 3.130 |
| 33 | 3.332 | 1.706 | 2.062 |
| 34 | 4.546 | 2.773 | 2.710 |
| 35 | 5.242 | 2.261 | 2.680 |
| 36 | 7.365 | 2.968 | 2.765 |
| 37 | 2.905 | 1.941 | 3.150 |
| 38 | 5.393 | 3.400 | 4.613 |
| 39 | 6.305 | 1.350 | 2.563 |
| 40 | 4.949 | 3.790 | 4.961 |
| 41 | 1.724 | 1.524 | 1.518 |
| 42 | 4.485 | 3.872 | 4.579 |

Table 3. Concluded

| Run | RMS pitch-attitude error, deg, for— | | |
|---|---|---|---|
| | Pilot 1 | Pilot 2 | Pilot 3 |
| 43 | 2.280 | 2.747 | 1.718 |
| 44 | 3.002 | 4.002 | 3.278 |
| 45 | 4.117 | 2.900 | 3.012 |
| 46 | 3.404 | 1.602 | 3.056 |
| 47 | 2.363 | 2.001 | 4.210 |
| 48 | 5.552 | 2.739 | 2.911 |
| 49 | 3.334 | 1.646 | 1.623 |
| 50 | 1.693 | 2.205 | 1.452 |
| 51 | 2.684 | 1.592 | 1.697 |
| 52 | 3.058 | 2.673 | 2.632 |
| 53 | 1.729 | 2.352 | 1.345 |
| 54 | 5.201 | 5.311 | 3.036 |
| 55 | 7.051 | 1.476 | 2.279 |
| 56 | 4.421 | 2.573 | 2.375 |
| 57 | 3.662 | 3.414 | 6.047 |
| 58 | 3.233 | 3.783 | 6.659 |
| 59 | 2.792 | 1.758 | 5.746 |
| 60 | 3.348 | 2.561 | 4.025 |
| 61 | 3.066 | 2.818 | 3.451 |
| 62 | 2.690 | 3.320 | 2.888 |
| 63 | 1.741 | 2.017 | 3.672 |
| 64 | 2.273 | 1.393 | 2.244 |
| 65 | 3.807 | 5.300 | 4.302 |
| 66 | 4.188 | 3.375 | 3.625 |
| 67 | 1.486 | 2.319 | 1.242 |
| 68 | 3.249 | 2.318 | 4.424 |
| 69 | 1.640 | 1.672 | 3.362 |
| 70 | 2.776 | 3.494 | 4.327 |
| 71 | 1.398 | 1.884 | 3.584 |
| 72 | 1.397 | 2.094 | 2.460 |
| 73 | 1.267 | 2.698 | 2.697 |
| 74 | 4.204 | 2.979 | 7.740 |
| 75 | 7.040 | 2.694 | 2.755 |
| 76 | 1.932 | .914 | 4.177 |
| 77 | 1.284 | 2.652 | 1.436 |
| 78 | 3.134 | 2.543 | 4.152 |
| 79 | 1.697 | 2.054 | 5.146 |
| 80 | 1.484 | 2.134 | 5.440 |
| 81 | 1.909 | 2.386 | 2.379 |
| 82 | 2.743 | 2.484 | 4.502 |
| 83 | 1.649 | 1.887 | 1.972 |
| 84 | 2.592 | 2.588 | 5.168 |

Table 4. Mean and Standard Deviation of Recovery Altitudes for Combinations of Shear and Strategy

| Shear | Statistic | Recovery altitude, ft, for strategy— | | |
|---|---|---|---|---|
| | | Pitch-hold | Acceleration | Flight-path angle |
| A90 | Mean . . . | 132.8 | 135.0 | 114.1 |
| | s.d. . . . . | 18.0 | 78.9 | 28.9 |
| A100 | Mean . . . | 57.2 | 35.3 | 73.0 |
| | s.d. . . . . | 39.3 | 44.7 | 38.3 |
| A110 | Mean . . . | 4.0 | 0 | 29.2 |
| | s.d. . . . . | 9.3 | 0 | 36.2 |
| B1.20 | Mean . . . | 125.6 | 166.7 | 149.4 |
| | s.d. . . . . | 46.9 | 87.0 | 43.6 |
| B1.25 | Mean . . . | 77.4 | 86.1 | 103.8 |
| | s.d. . . . . | 58.4 | 98.4 | 65.3 |
| B1.30 | Mean . . . | 58.4 | 51.8 | 35.8 |
| | s.d. . . . . | 59.1 | 70.9 | 56.3 |
| ALOW | Mean . . . | 103.0 | 100.7 | 102.8 |
| | s.d. . . . . | 37.9 | 69.6 | 18.1 |
| All shears | Mean . . . | 79.8 | 82.2 | 86.9 |
| | s.d. . . . . | 58.4 | 87.2 | 58.3 |

Table 5. Mean and Standard Deviation of RMS Pitch-Attitude Error for Combinations of Shear and Strategy

| Shear | Statistic | Pitch-attitude error, deg, for strategy— | | |
|---|---|---|---|---|
| | | Pitch-hold | Acceleration | Flight-path angle |
| A90 | Mean . . . | 1.91 | 1.98 | 1.89 |
| | s.d. . . . . | .46 | .67 | .56 |
| A100 | Mean . . . | 3.61 | 2.53 | 2.31 |
| | s.d. . . . . | 1.70 | 1.11 | .75 |
| A110 | Mean . . . | 2.86 | 2.88 | 2.13 |
| | s.d. . . . . | 1.15 | .81 | .66 |
| B1.20 | Mean . . . | 4.32 | 3.27 | 2.93 |
| | s.d. . . . . | 1.17 | .47 | .78 |
| B1.25 | Mean . . . | 5.06 | 4.00 | 3.61 |
| | s.d. . . . . | 1.36 | 1.26 | 1.54 |
| B1.30 | Mean . . . | 4.06 | 3.91 | 3.66 |
| | s.d. . . . . | 1.30 | 1.01 | 1.05 |
| ALOW | Mean . . . | 3.05 | 2.50 | 1.88 |
| | s.d. . . . . | 2.16 | 1.25 | .34 |
| All shears | Mean . . . | 3.55 | 3.01 | 2.63 |
| | s.d. . . . . | 1.67 | 1.18 | 1.12 |

Table 6. Analysis of Variance of Recovery Altitude for Factors Strategies and Shears

| Source of variation | Sum of squares | Degrees of freedom | Mean square | Computed $f$-value | $F$-value at level of significance of— | |
|---|---|---|---|---|---|---|
| | | | | | 0.05 | 0.01 |
| Strategy . . . . | 2531.9 | 2 | 1266.0 | 0.4 | 3.0 | 4.7 |
| Shear . . . . . | 474847.4 | 5 | 94969.5 | 31.4 | 2.2 | 3.1 |
| Interaction . . . | 33093.8 | 10 | 3309.4 | 1.1 | 1.9 | 2.4 |
| Error . . . . . | 599312.9 | 198 | 3026.8 | | | |
| Total . . . . . | 1109786.0 | | | | | |
| Conclusions: There is no interaction between factors. There is no difference in recovery altitude between recovery strategies. There is a difference in recovery altitude between shears. | | | | | | |

Table 7. Analysis of Variance of Recovery Altitude for Factors Strategies and Pilots

| Source of variation | Sum of squares | Degrees of freedom | Mean square | Computed $f$-value | $F$-value at level of significance of— | |
|---|---|---|---|---|---|---|
| | | | | | 0.05 | 0.01 |
| Strategy . . . . | 2531.9 | 2 | 1266.0 | 0.3 | 3.0 | 4.7 |
| Pilot . . . . . | 119783.1 | 2 | 59891.6 | 12.8 | 3.0 | 4.7 |
| Interaction . . . | 17525.4 | 4 | 4381.4 | 0.9 | 2.4 | 3.4 |
| Error . . . . . | 969945.6 | 207 | 4685.7 | | | |
| Total . . . . . | 1109786.0 | | | | | |
| Conclusions: There is no interaction between factors. There is no difference in recovery altitude between recovery strategies. There is a difference in recovery altitude between pilots. | | | | | | |

Table 8. Analysis of Variance of Recovery Altitude for Each Shear Type for the Factor Strategy

| Shear | Source of variation | Sum of squares | Degrees of freedom | Mean square | Computed $f$-value | $F$-value at level of significance of— 0.05 | 0.01 |
|---|---|---|---|---|---|---|---|
| A90 | Strategy | 3173.5 | 2 | 1586.8 | 0.7 | 3.3 | 5.4 |
| | Error | 81169.5 | 33 | 2459.7 | | | |
| | Total | 84343.0 | | | | | |
| A100 | Strategy | 8604.1 | 2 | 4302.1 | 2.6 | 3.3 | 5.4 |
| | Error | 55120.3 | 33 | 1670.3 | | | |
| | Total | 63724.4 | | | | | |
| A110 | Strategy | 6029.9 | 2 | 3015.0 | 6.5 | 3.3 | 5.4 |
| | Error | 15345.9 | 33 | 465.0 | | | |
| | Total | 21375.8 | | | | | |
| B1.20 | Strategy | 10234.5 | 2 | 5117.3 | 1.3 | 3.3 | 5.4 |
| | Error | 128329.6 | 33 | 3888.8 | | | |
| | Total | 138564.1 | | | | | |
| B1.25 | Strategy | 4332.1 | 2 | 2166.1 | 0.4 | 3.3 | 5.4 |
| | Error | 190822.5 | 33 | 5782.5 | | | |
| | Total | 195154.6 | | | | | |
| B1.30 | Strategy | 3251.7 | 2 | 1625.9 | 0.4 | 3.3 | 5.4 |
| | Error | 128525.1 | 33 | 3894.7 | | | |
| | Total | 131776.8 | | | | | |

Conclusion:
There is no difference in recovery altitude between recovery strategies for all shears except shear A110, where a difference exists.

Table 9. Analysis of Variance of RMS Pitch-Attitude Error for Factors Strategies and Shears

| Source of variation | Sum of squares | Degrees of freedom | Mean square | Computed $f$-value | $F$-value at level of significance of— 0.05 | 0.01 |
|---|---|---|---|---|---|---|
| Strategy | 28.049 | 2 | 14.025 | 12.7 | 3.0 | 4.7 |
| Shear | 133.178 | 5 | 26.636 | 24.1 | 2.2 | 3.1 |
| Interaction | 14.514 | 10 | 1.451 | 1.31 | 1.9 | 2.4 |
| Error | 218.201 | 198 | 1.102 | | | |
| Total | 1109786.0 | | | | | |

Conclusions:
There is no interaction between factors.
There is a difference in RMS pitch error between recovery strategies.
There is a difference in RMS pitch error between shears.

Table 10. Analysis of Variance of RMS Pitch-Attitude Error for Factors Strategies and Pilots

| Source of variation | Sum of squares | Degrees of freedom | Mean square | Computed $f$-value | $F$-value at level of significance of— | |
|---|---|---|---|---|---|---|
| | | | | | 0.05 | 0.01 |
| Strategy . . . . | 28.6 | 2 | 14.3 | 8.4 | 3.0 | 4.7 |
| Pilot . . . . . | 21.9 | 2 | 11.0 | 6.5 | 3.0 | 4.7 |
| Interaction . . . | 1.0 | 4 | 0.3 | 0.2 | 2.4 | 3.4 |
| Error . . . . . | 343.5 | 207 | 1.7 | | | |
| Total . . . . . | 395.0 | | | | | |
| Conclusions: There is no interaction between factors. There is a difference in RMS pitch error between recovery strategies. There is a difference in RMS pitch error between pilots. | | | | | | |

Table 11. Comparison of Recovery Altitudes in Batch and Real-Time Simulations

(a) Batch simulation

| $\Delta Wx$, knots | Recovery altitude, ft, for strategy— | | | | | | | | | | | | | |
|---|---|---|---|---|---|---|---|---|---|---|---|---|---|---|
| | Pitch-hold with target, deg, of— | | | | | | | Acceleration with gain of— | | | | Flight-path angle with gain of— | | |
| | 10 | 11 | 12 | 13 | 14 | 15 | 16 | 0.1 | 0.2 | 0.3 | 0.4 | 0.65 | 0.75 | 0.85 |
| 90 | 77 | 110 | 140 | 169 | 194 | 212 | 220 | 26 | 137 | 241 | 231 | 104 | 104 | 104 |
| 100 | 37 | 65 | 92 | 114 | 128 | 129 | 108 | 0 | 57 | 152 | 77 | 102 | 103 | 102 |
| 110 | 0 | 21 | 39 | 46 | 38 | 10 | 0 | 0 | 0 | 53 | 0 | 101 | 100 | 101 |

(b) Real-time simulation

| $\Delta Wx$, knots | Recovery altitude, ft, for strategy— | | | |
|---|---|---|---|---|
| | Pitch-hold with 13° target | | Acceleration with gain of 0.2 | Flight-path angle with gain of 0.75 |
| 90 | Mean . . . | 133 | 135 | 114 |
| | s.d. . . . . | 18 | 79 | 29 |
| 100 | Mean . . . | 57 | 35 | 73 |
| | s.d. . . . . | 39 | 45 | 38 |
| 110 | Mean . . . | 4 | 0 | 29 |
| | s.d. . . . . | 9 | 0 | 36 |

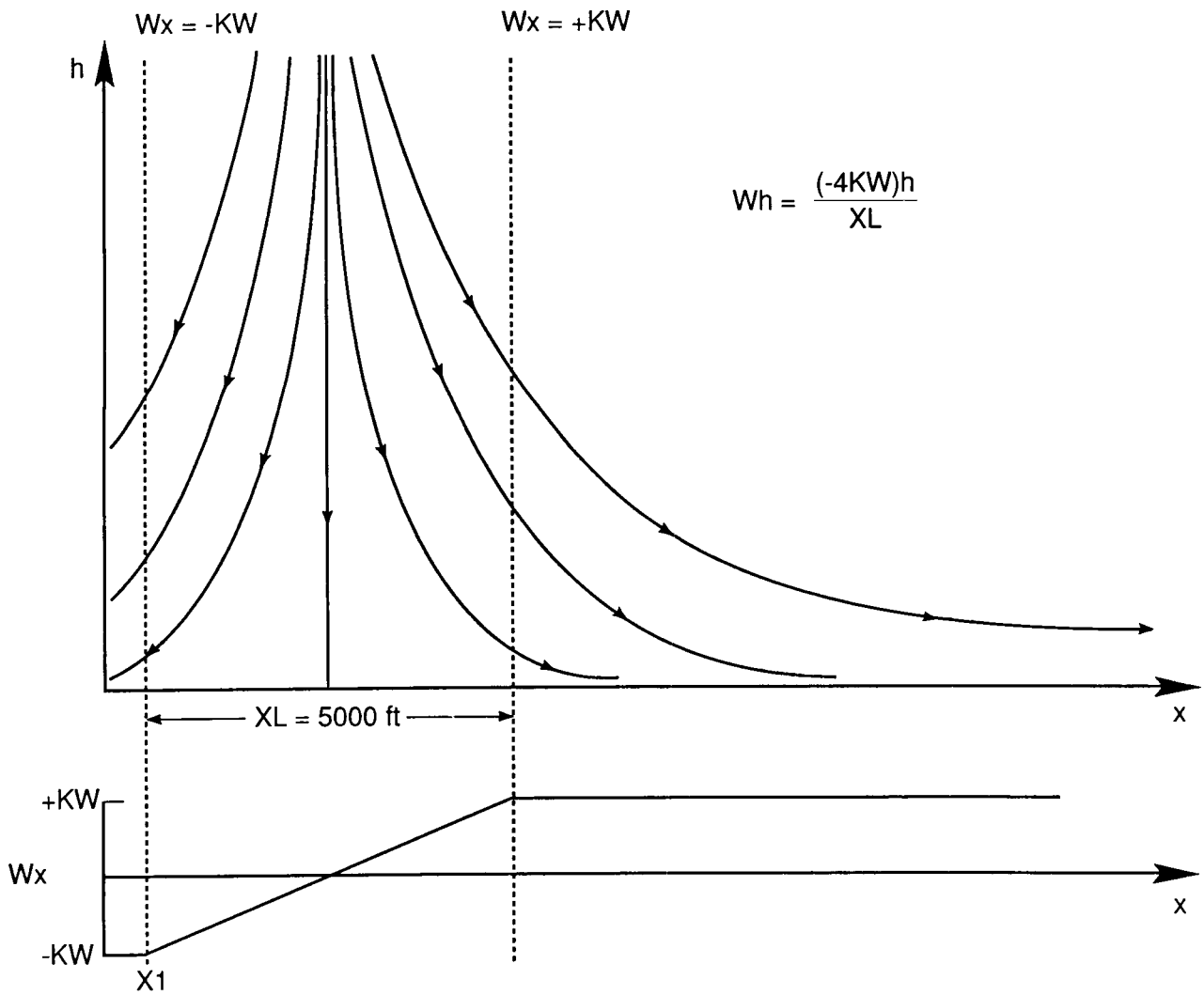


Figure 1. Wind shear model A.

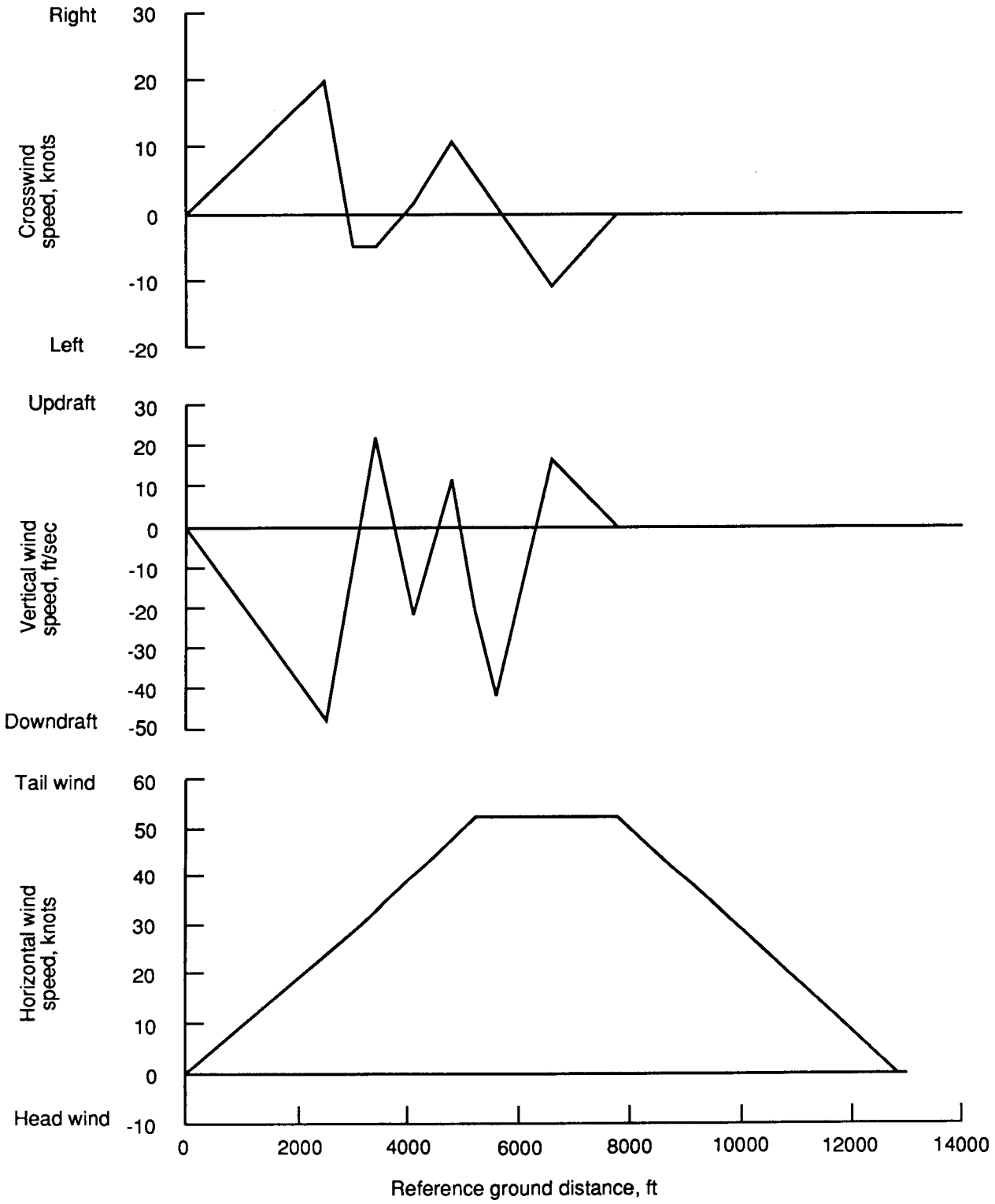


Figure 2. Wind components for shear B.

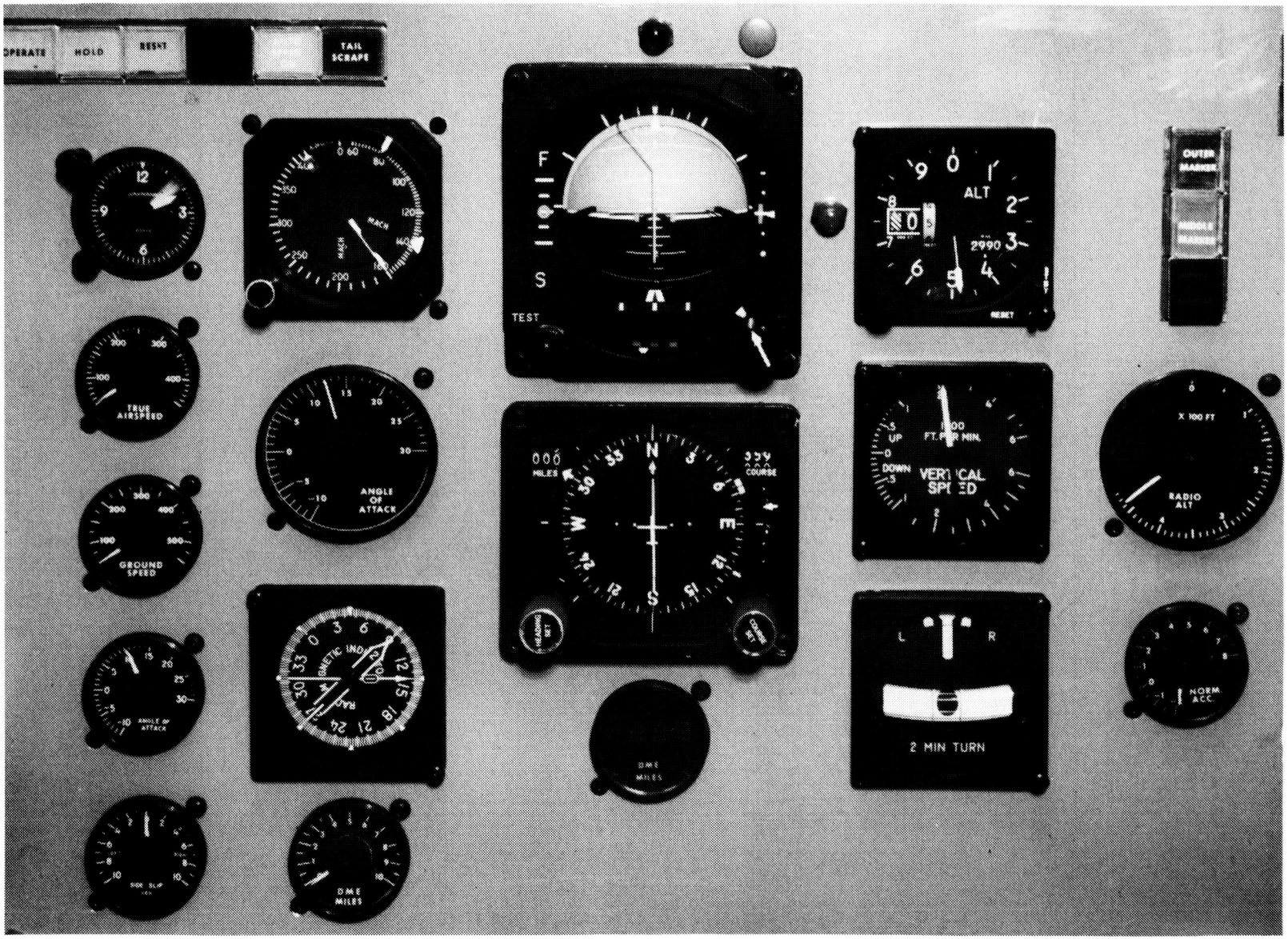


L-87-5712

Figure 3. Flight instrumentation in the Langley Visual Motion Simulator.

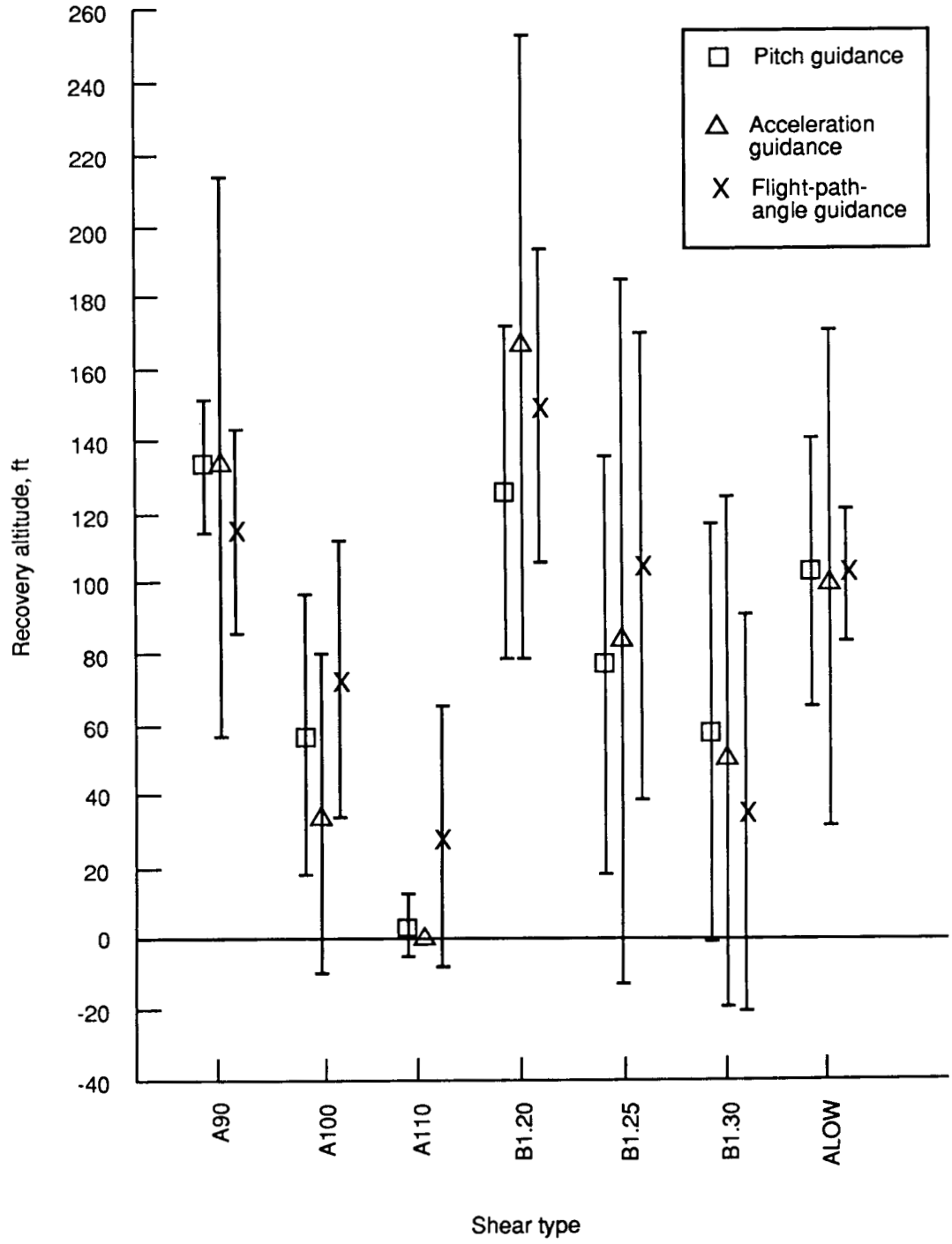


Figure 4. Mean and standard deviation of recovery altitude in real-time simulation.

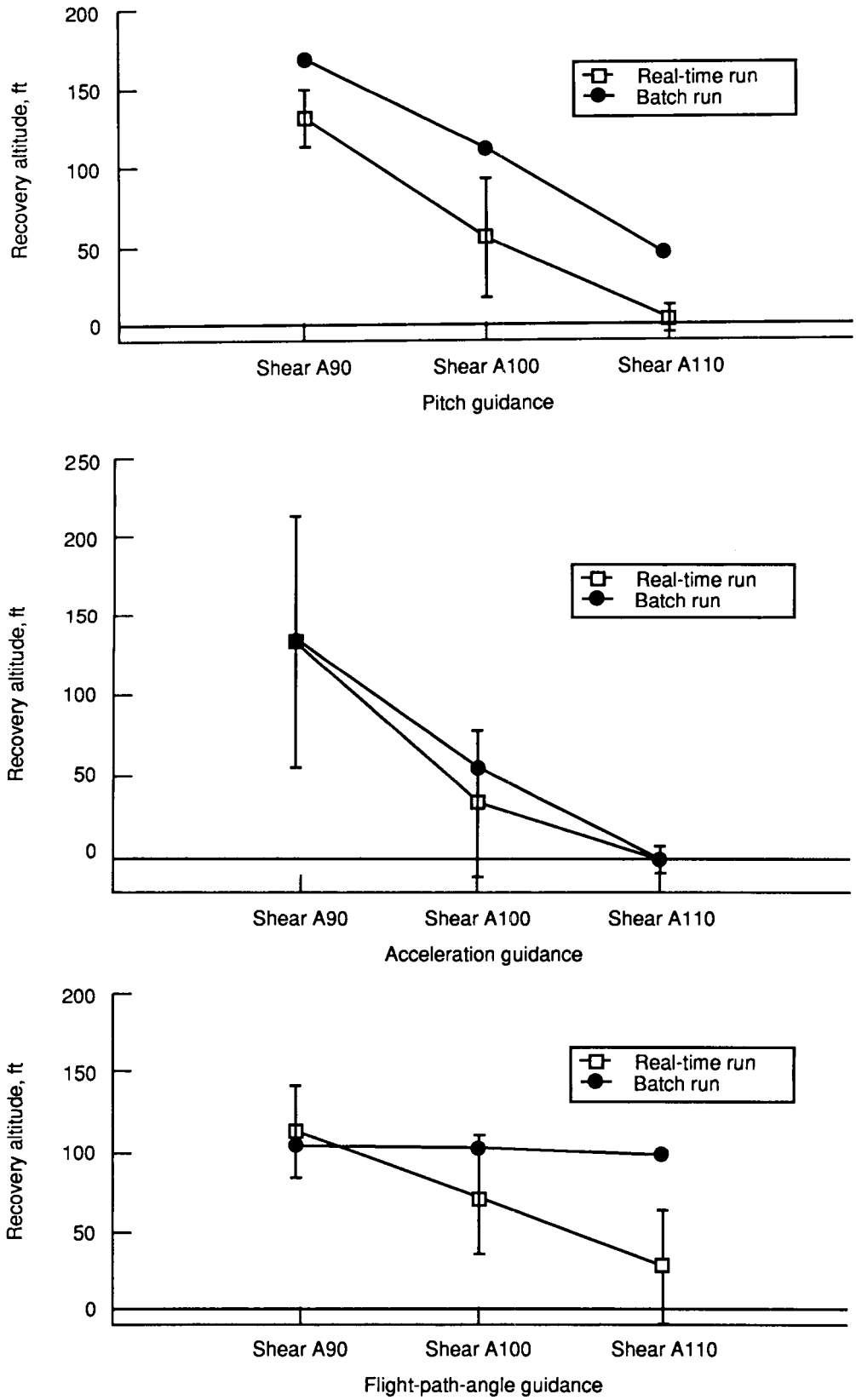


Figure 5. Comparison of recovery altitudes in batch and real-time simulations.

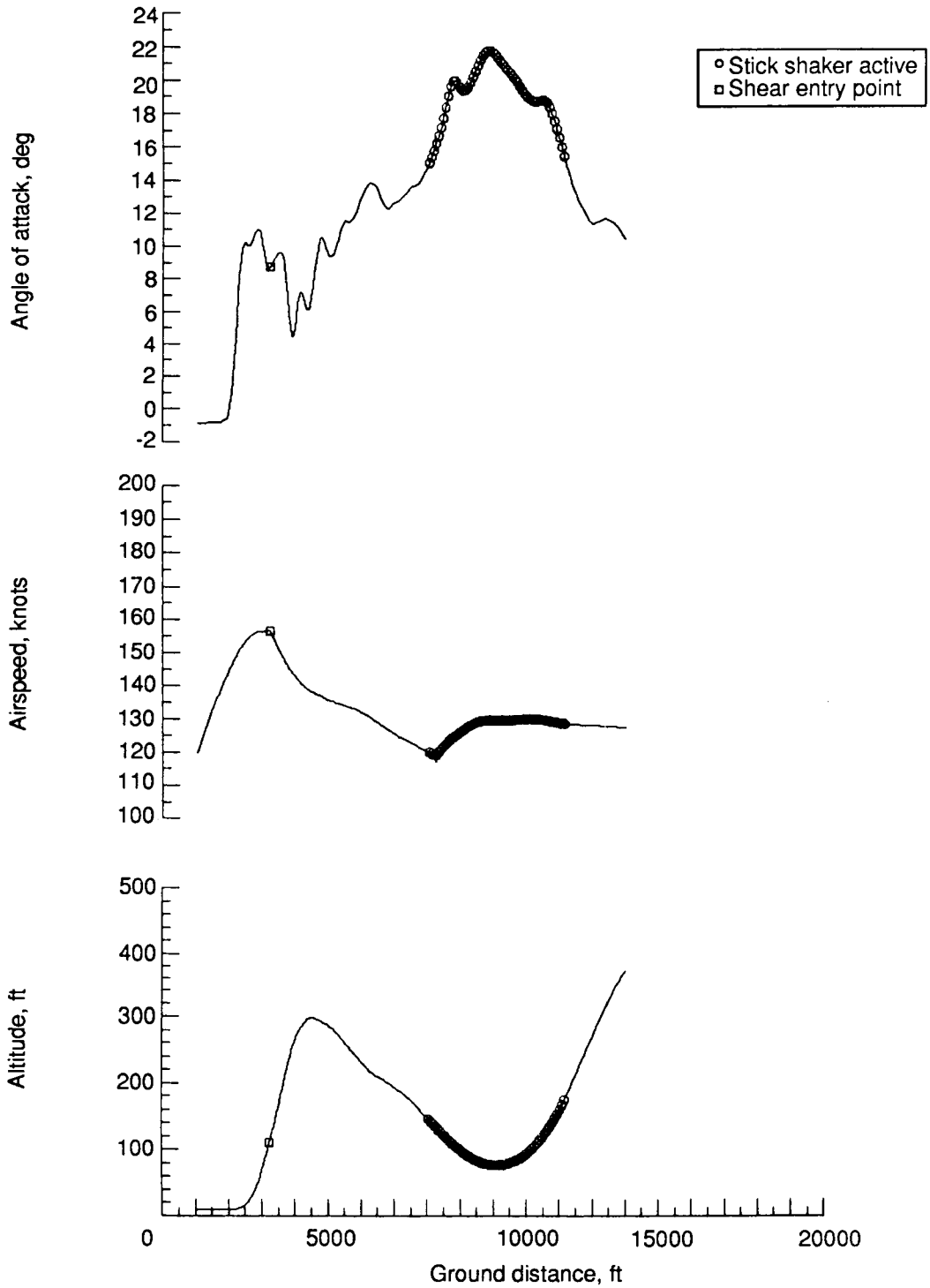


(a) Altitude, airspeed, and angle of attack.

Figure 6. Piloted recovery from shear A100 with pitch guidance.

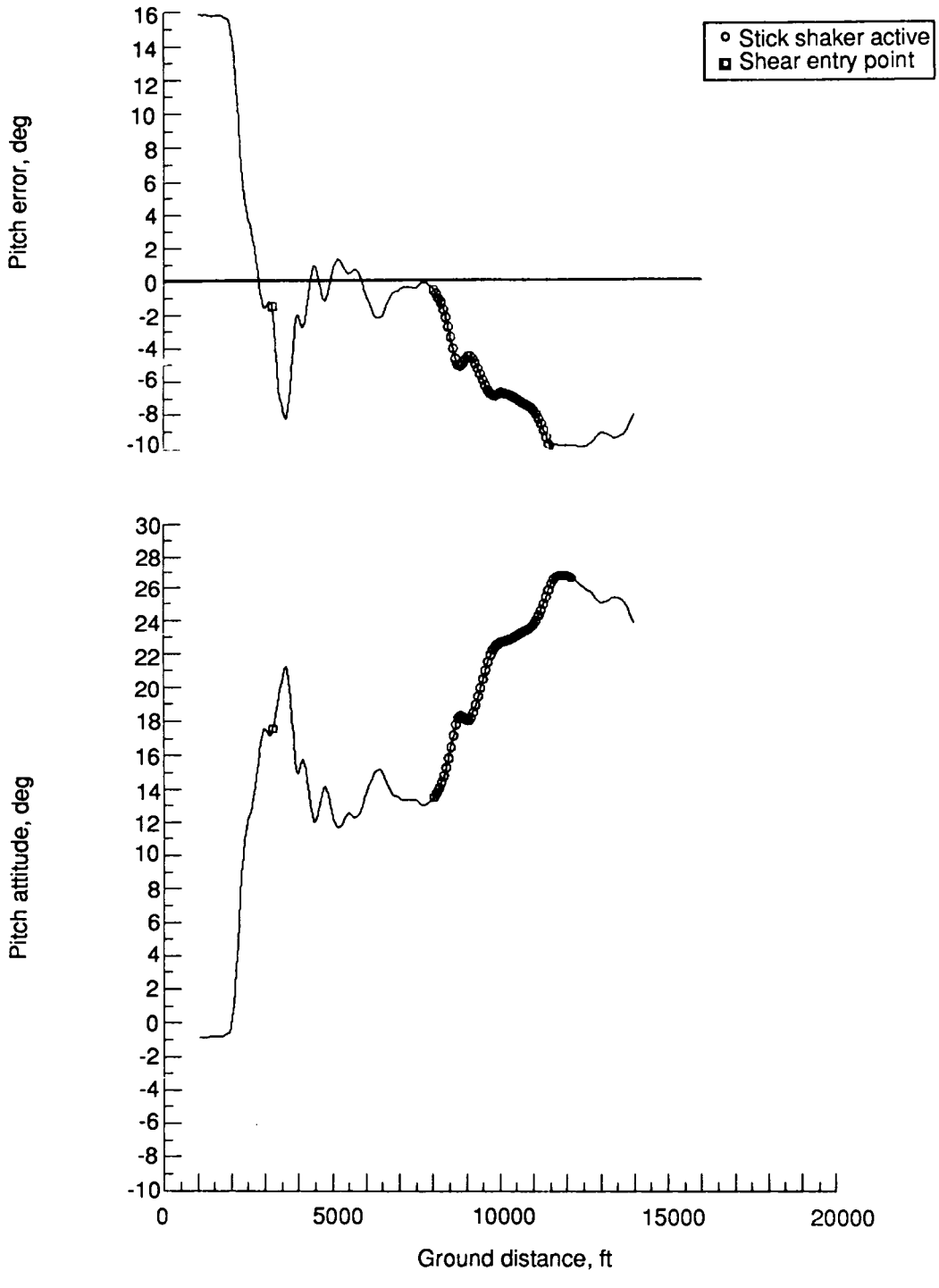


(b) Pitch attitude and error.

Figure 6. Concluded.

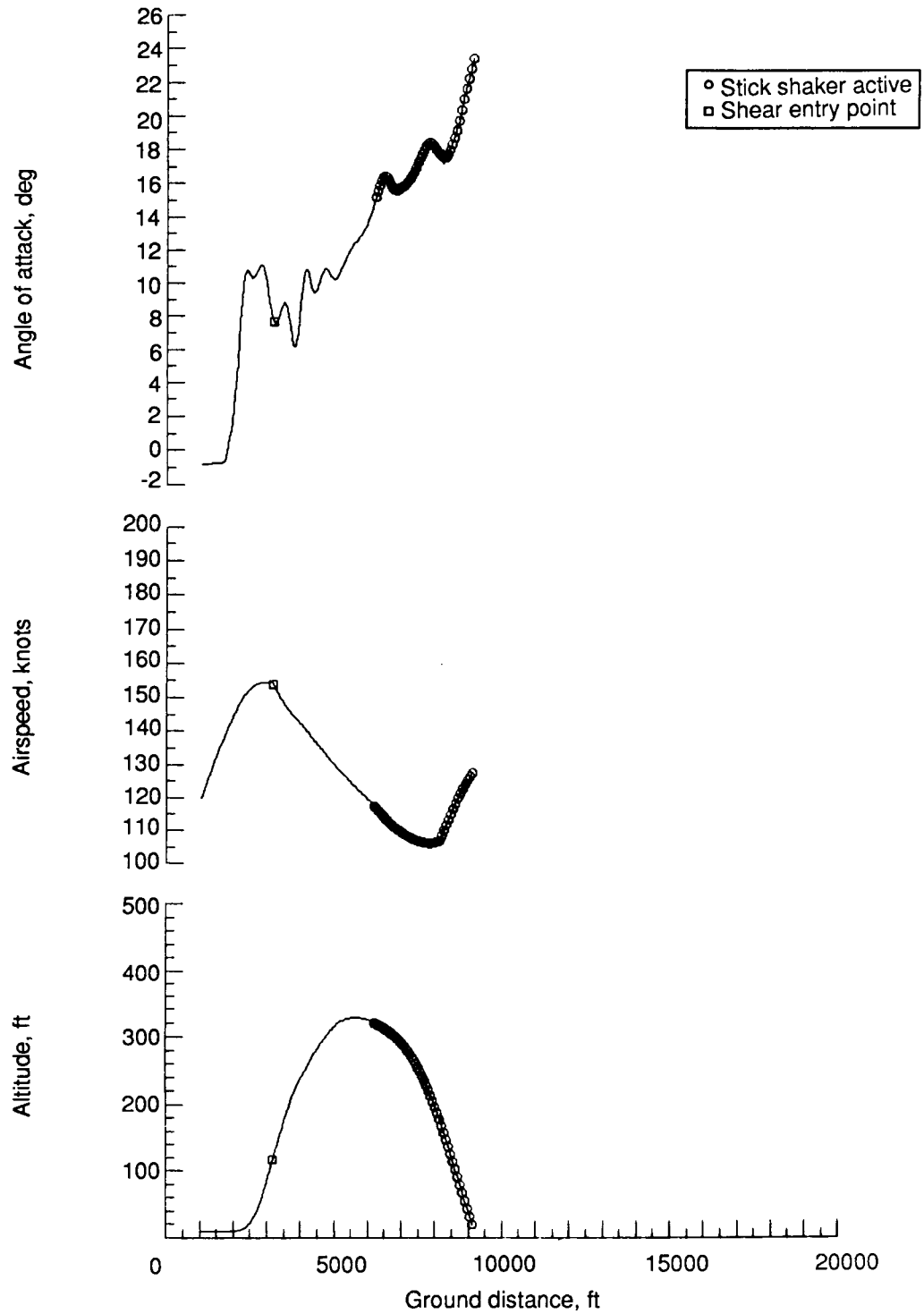


(a) Altitude, airspeed, and angle of attack.

Figure 7. Piloted recovery from shear A100 with acceleration guidance.

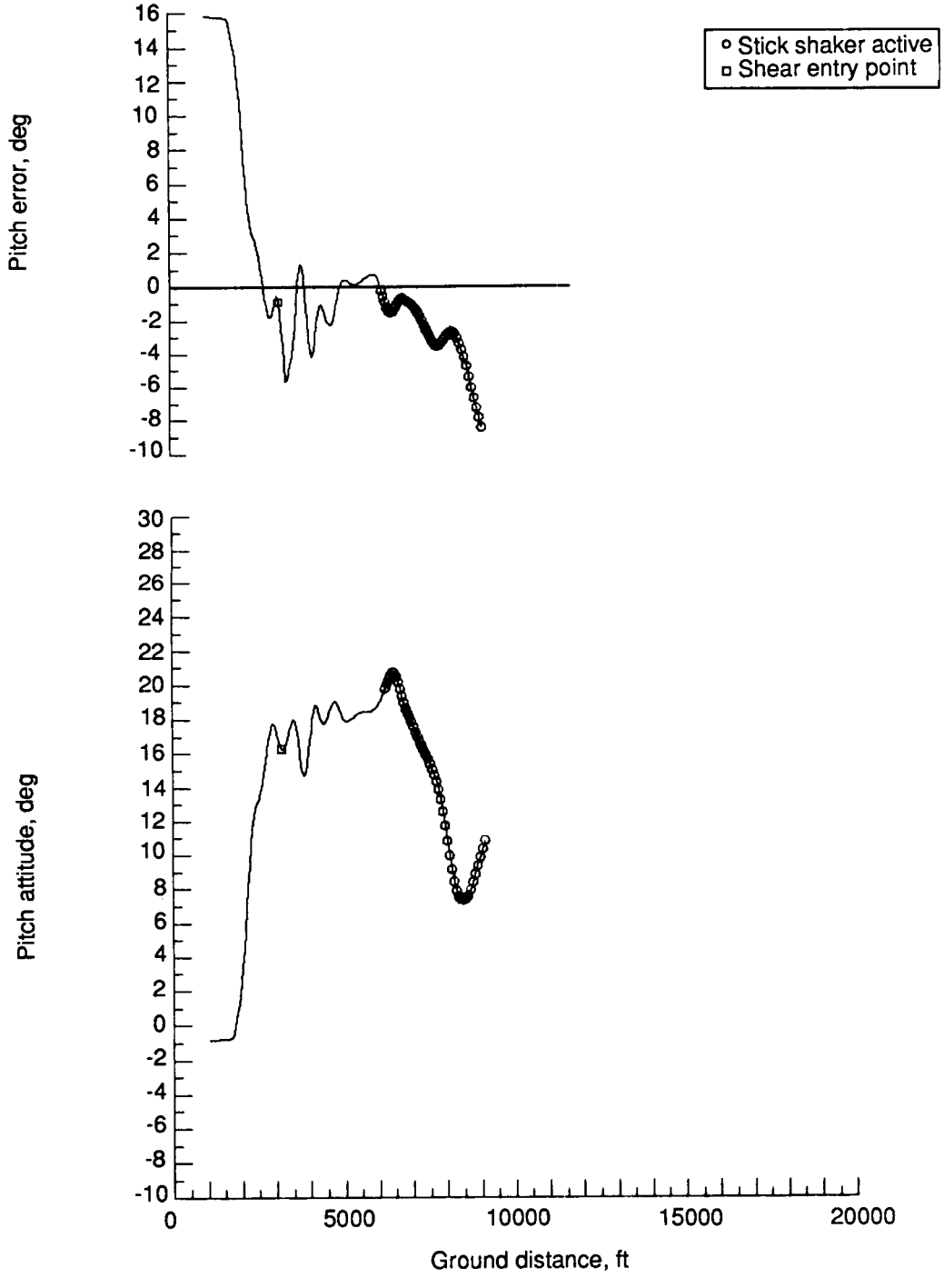


(b) Pitch attitude and error.

Figure 7. Concluded.

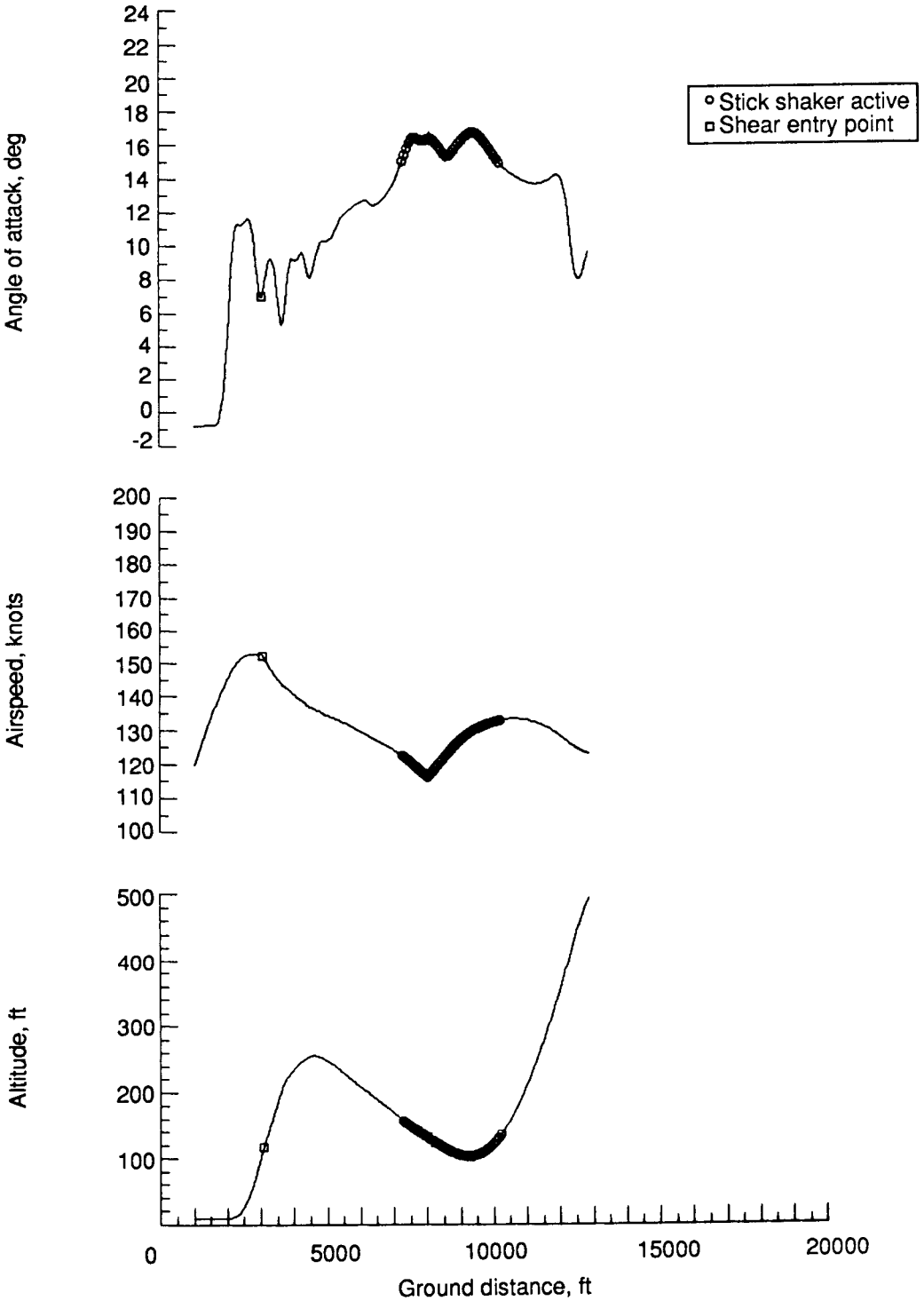


(a) Altitude, airspeed, and angle of attack.

Figure 8. Piloted recovery from shear A100 with flight-path guidance.

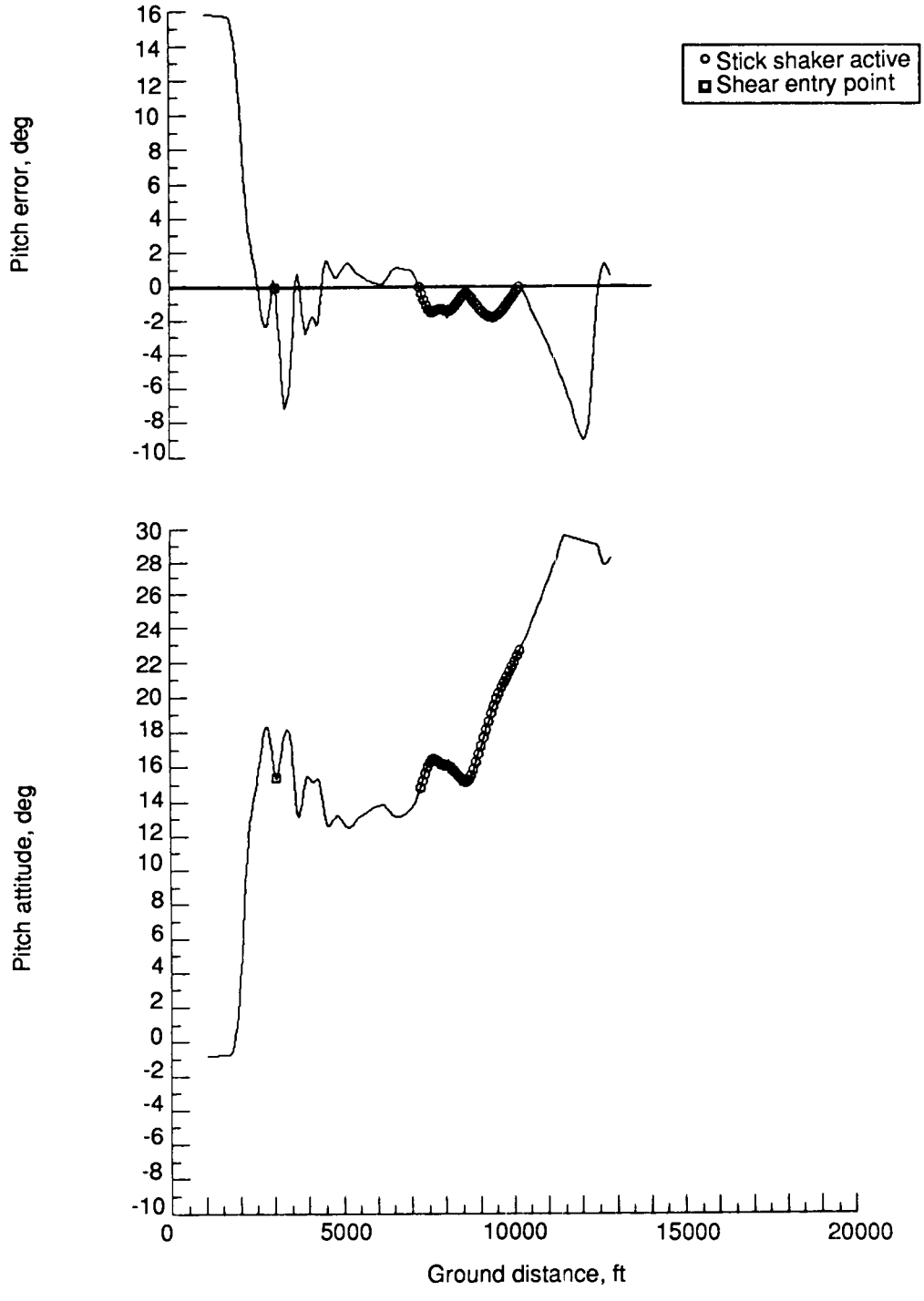


(b) Pitch attitude and error.

Figure 8. Concluded.

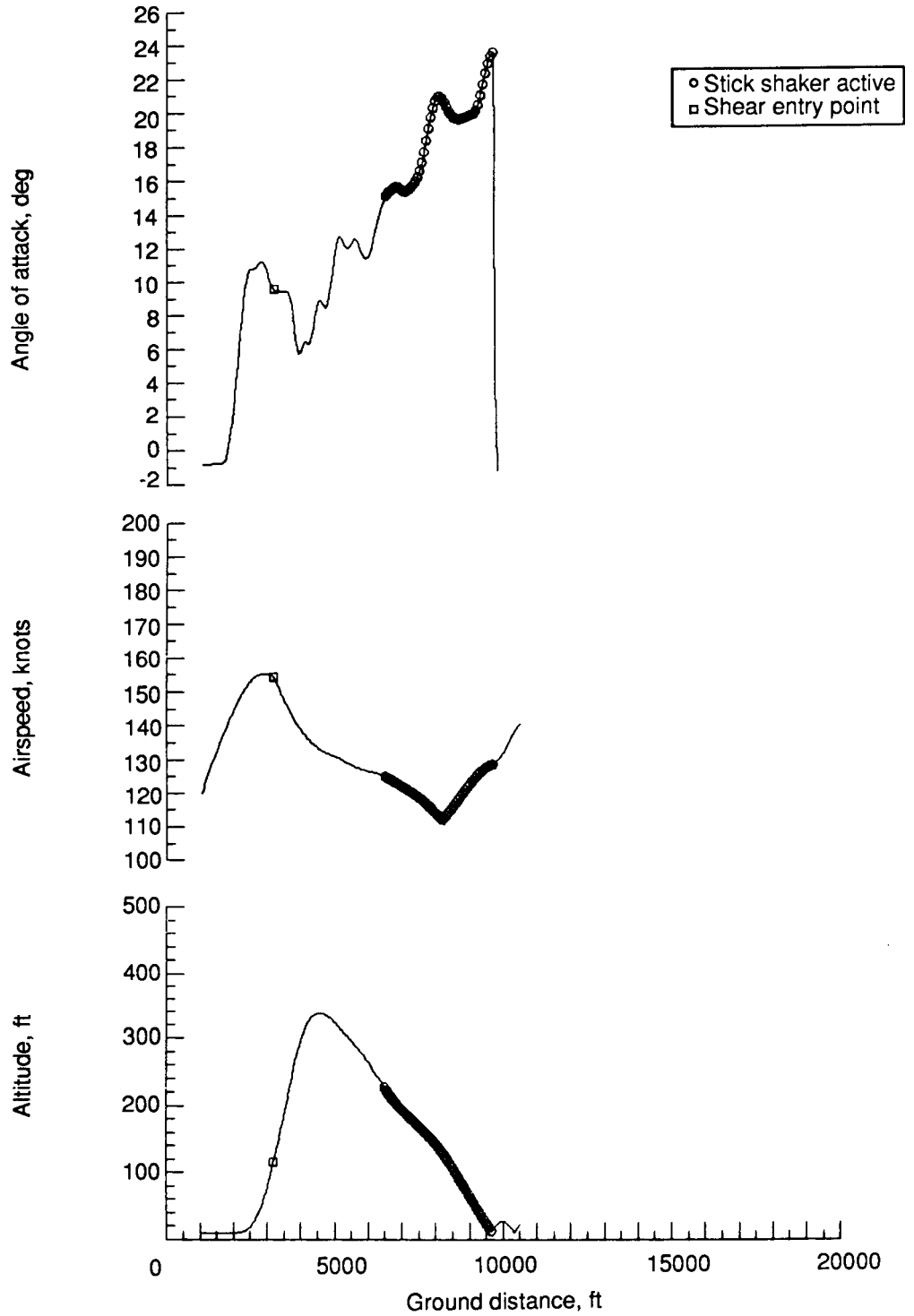


(a) Altitude, airspeed, and angle of attack.

Figure 9. Shear A100 encounter flown with excess pitch attitude.

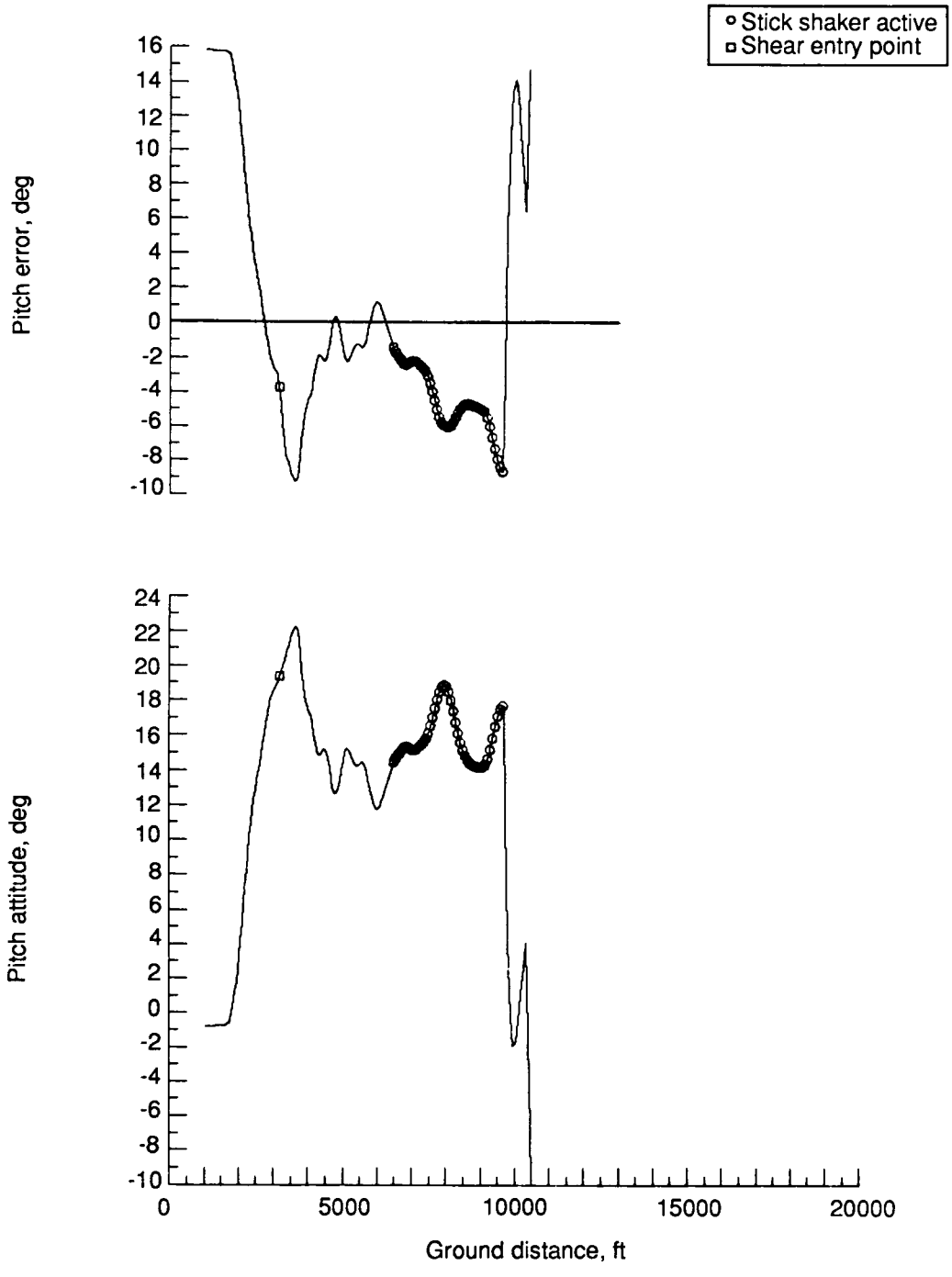


(b) Pitch attitude and error.

Figure 9. Concluded.

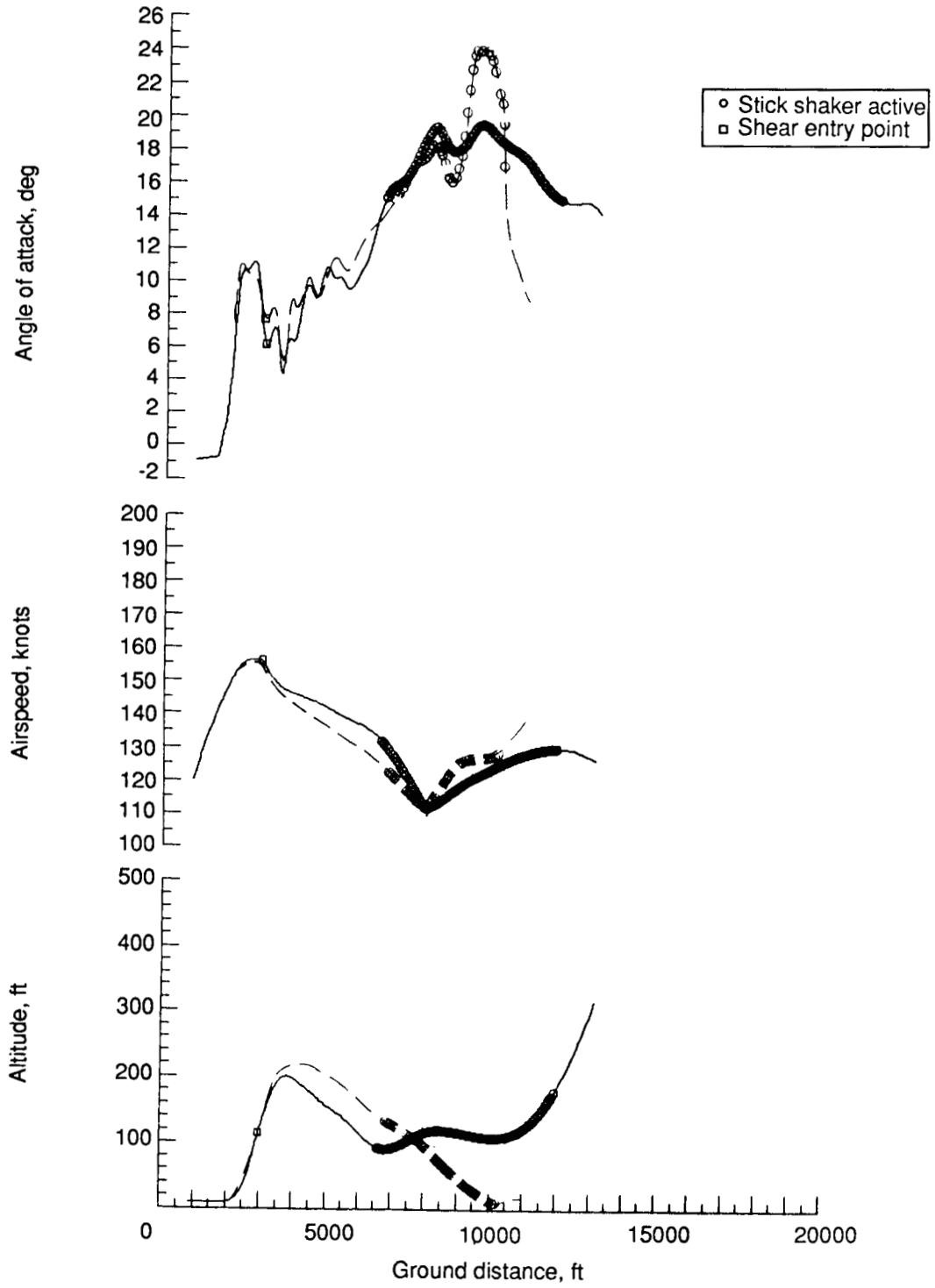


(a) Altitude, airspeed, and angle of attack.

Figure 10. Comparison of two recoveries in shear A110 with flight-path guidance.

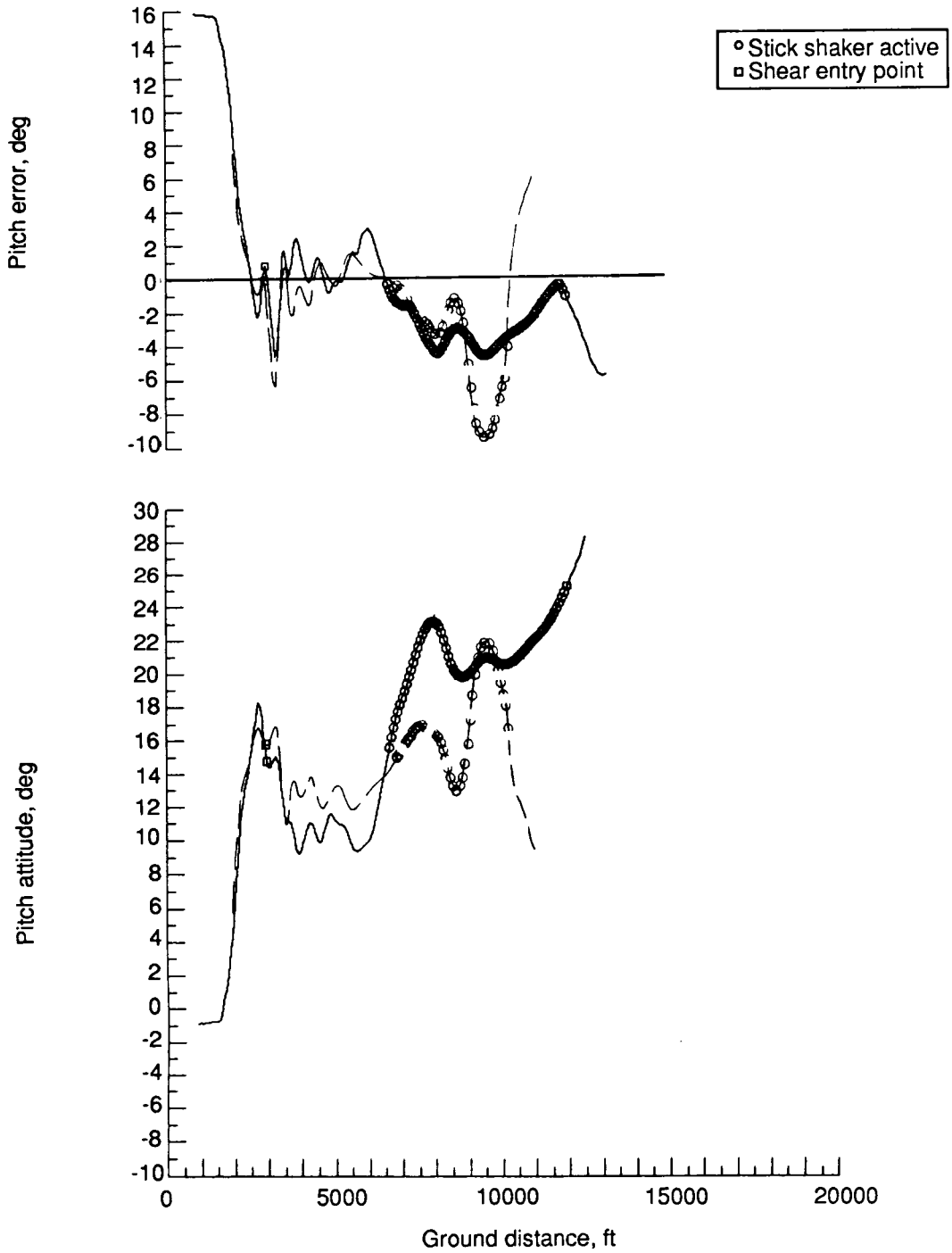


(b) Pitch attitude and error.

Figure 10. Concluded.

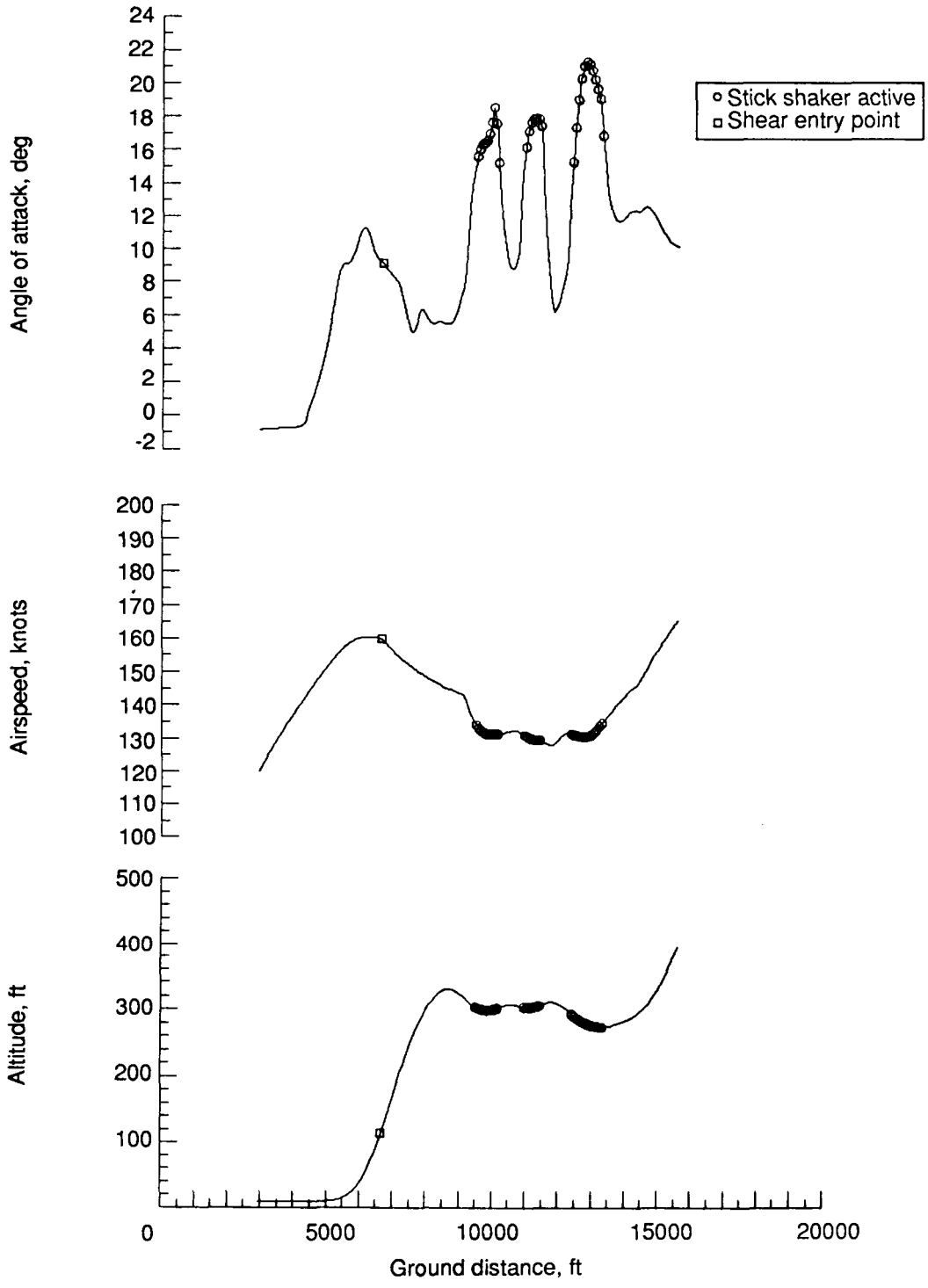


(a) Altitude, airspeed, and angle of attack.

Figure 11. Recovery from shear B1.25 with acceleration guidance.

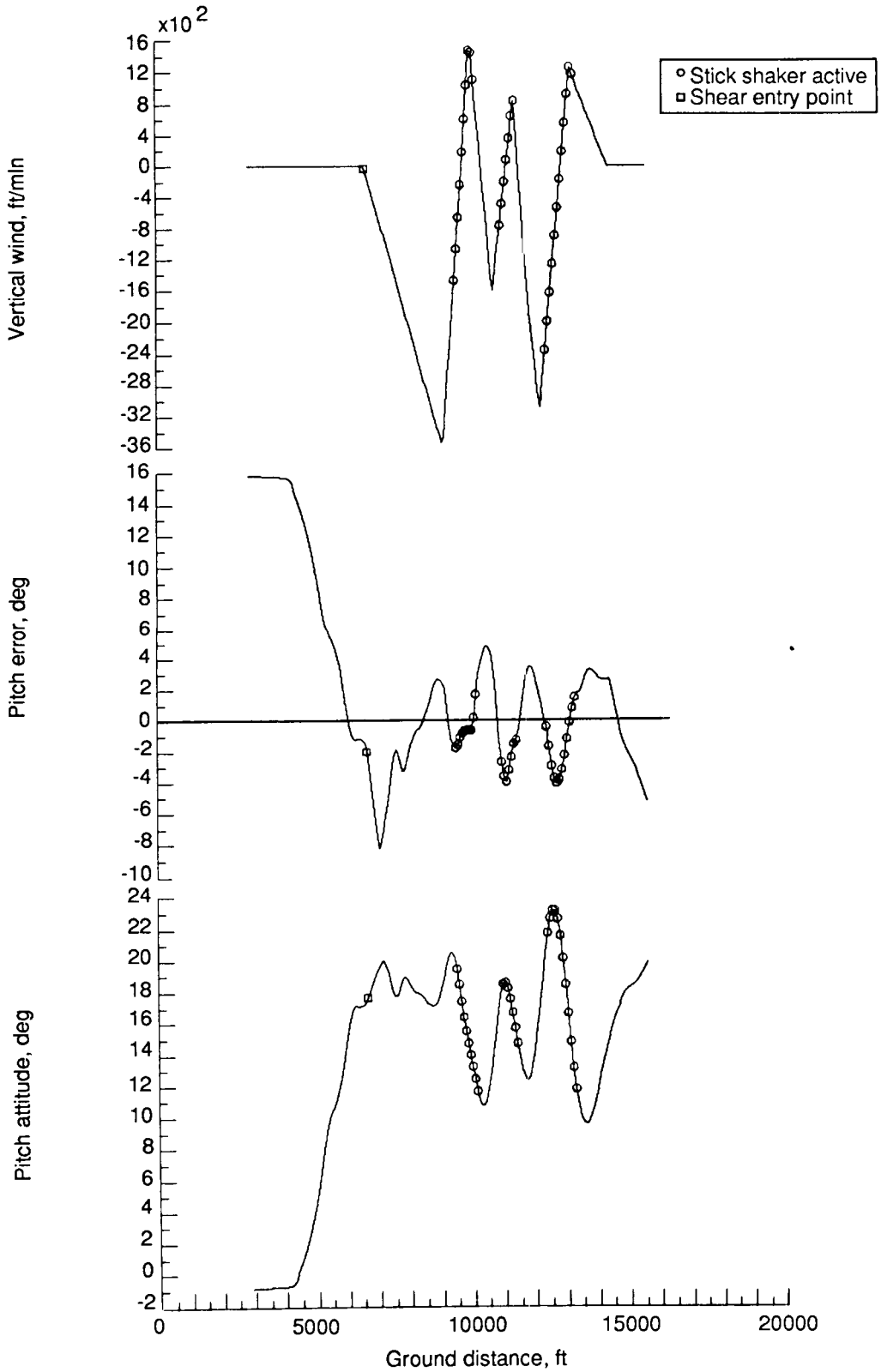


(b) Pitch attitude, pitch error, and vertical wind.

Figure 11. Concluded.

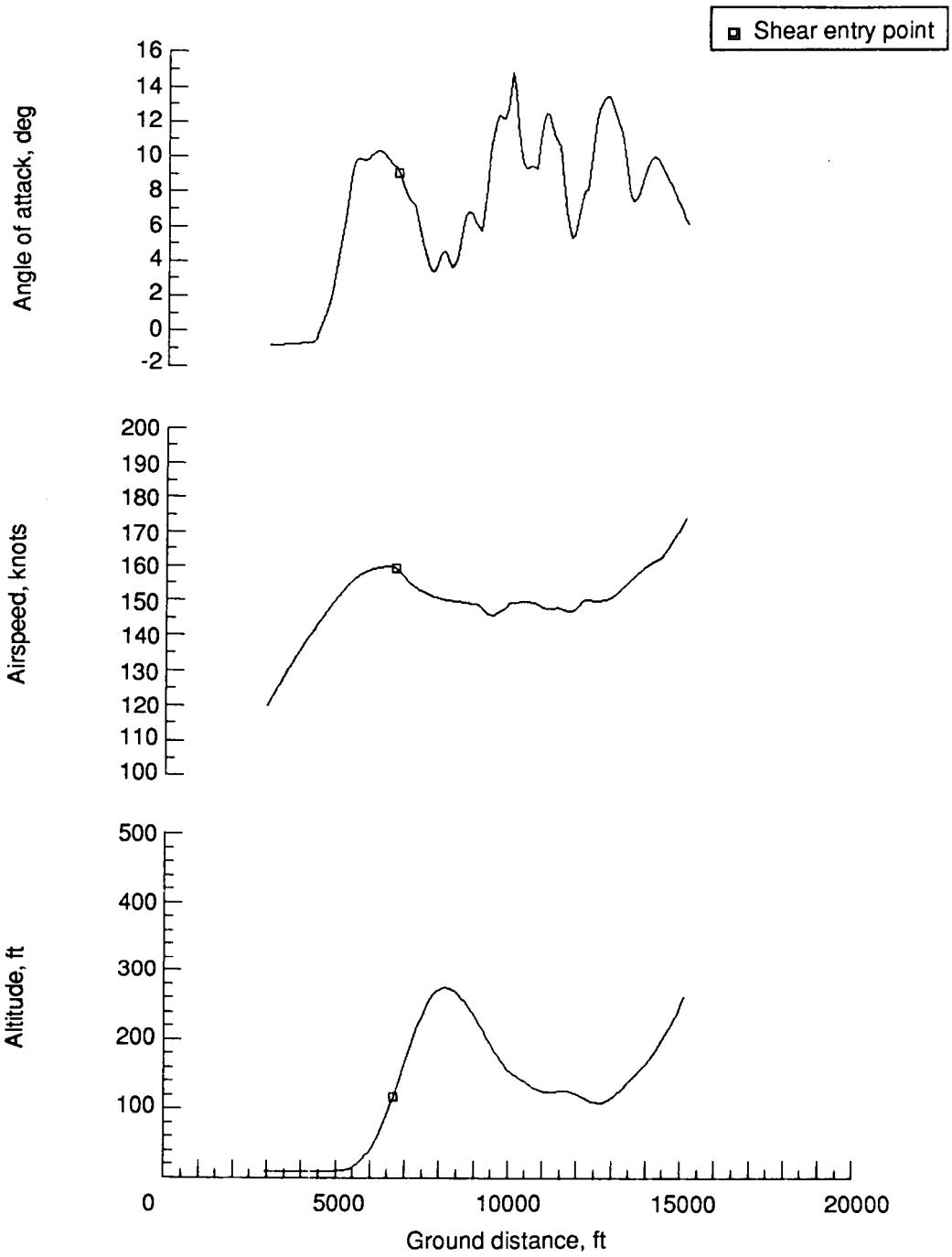


(a) Altitude, airspeed, and angle of attack.

Figure 12. Recovery from shear B1.20 without stick-shaker activation.

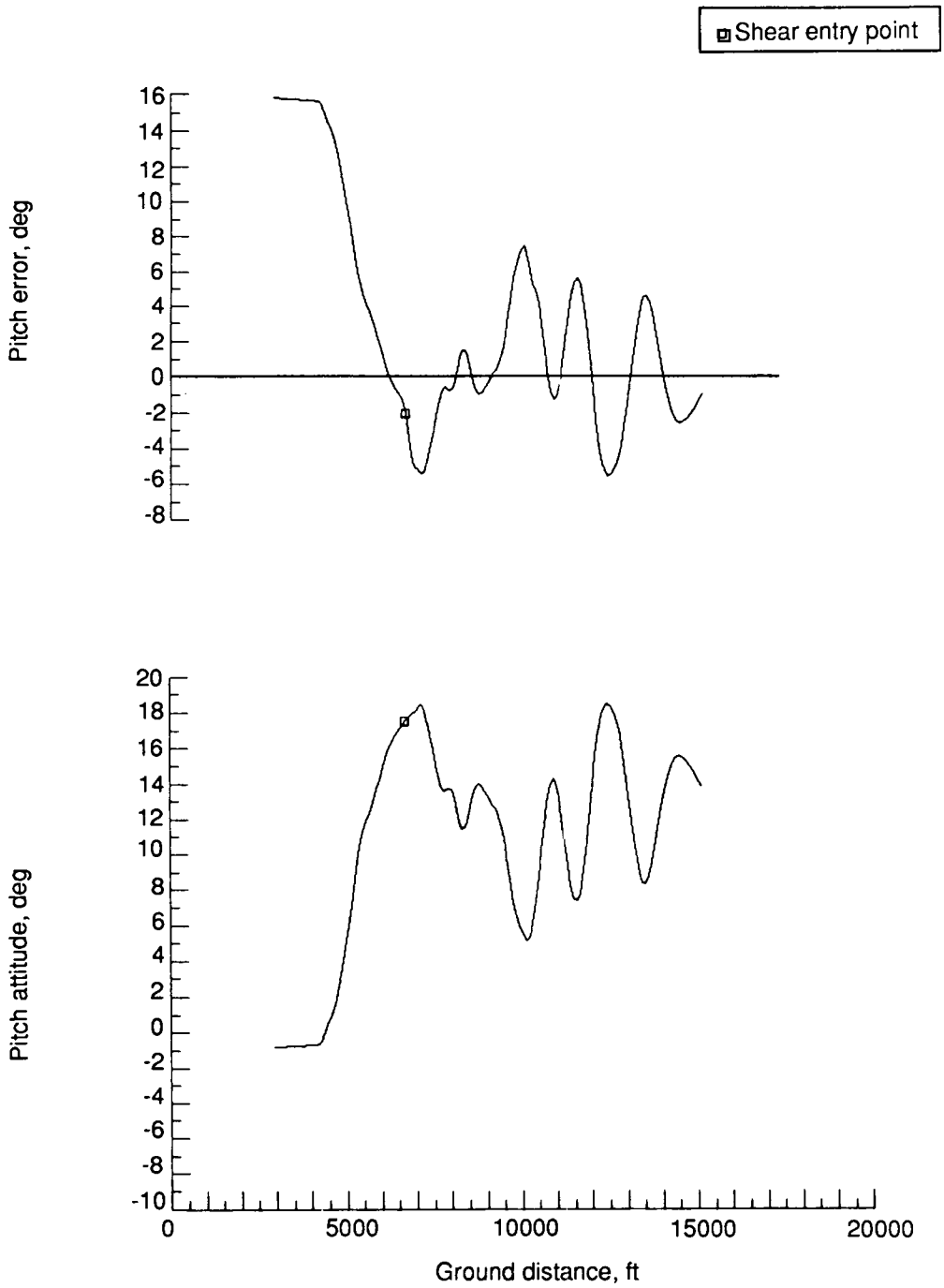


(b) Pitch attitude and error.

Figure 12. Continued.

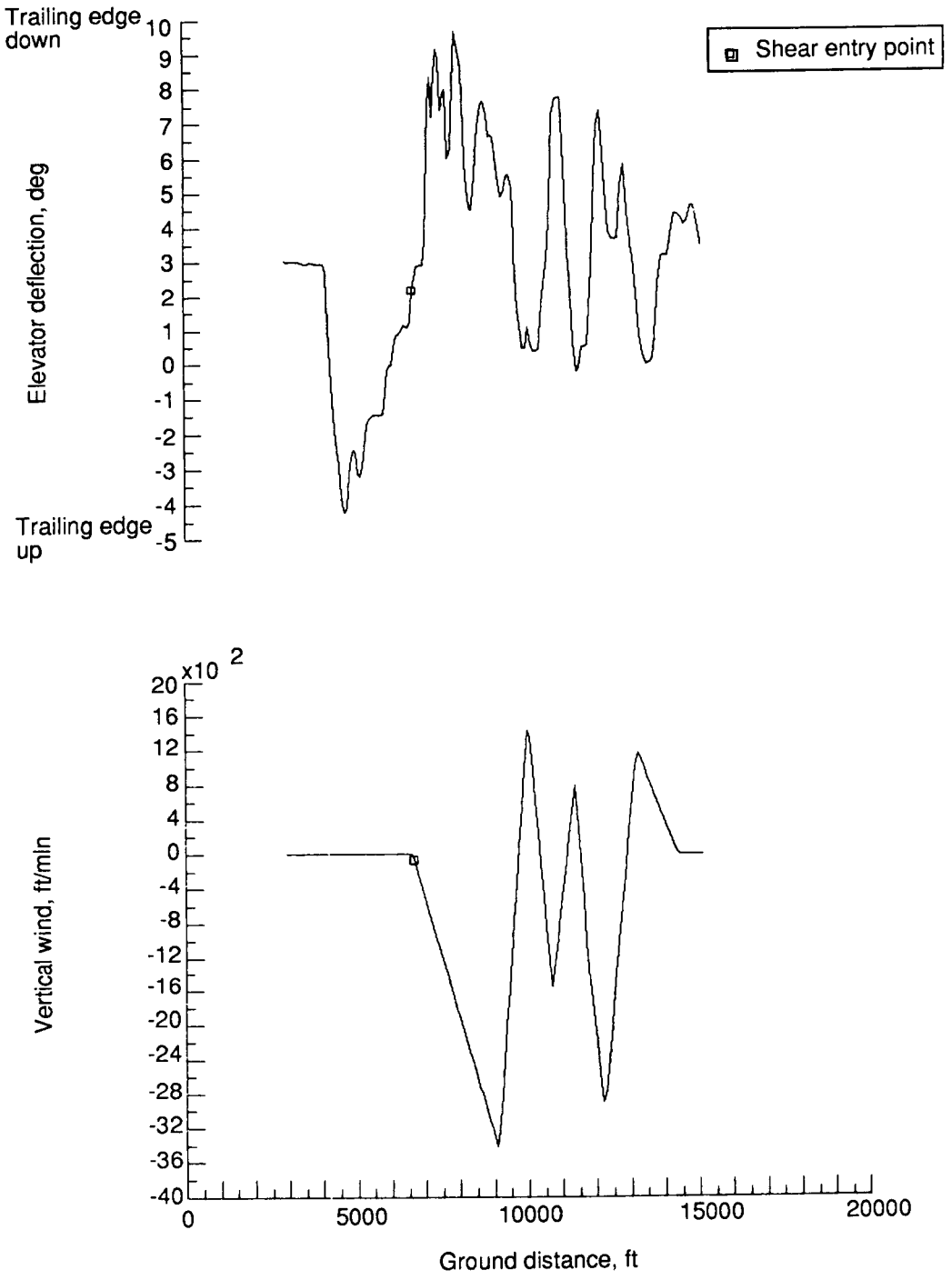


(c) Vertical wind and elevator deflection.

Figure 12. Concluded.

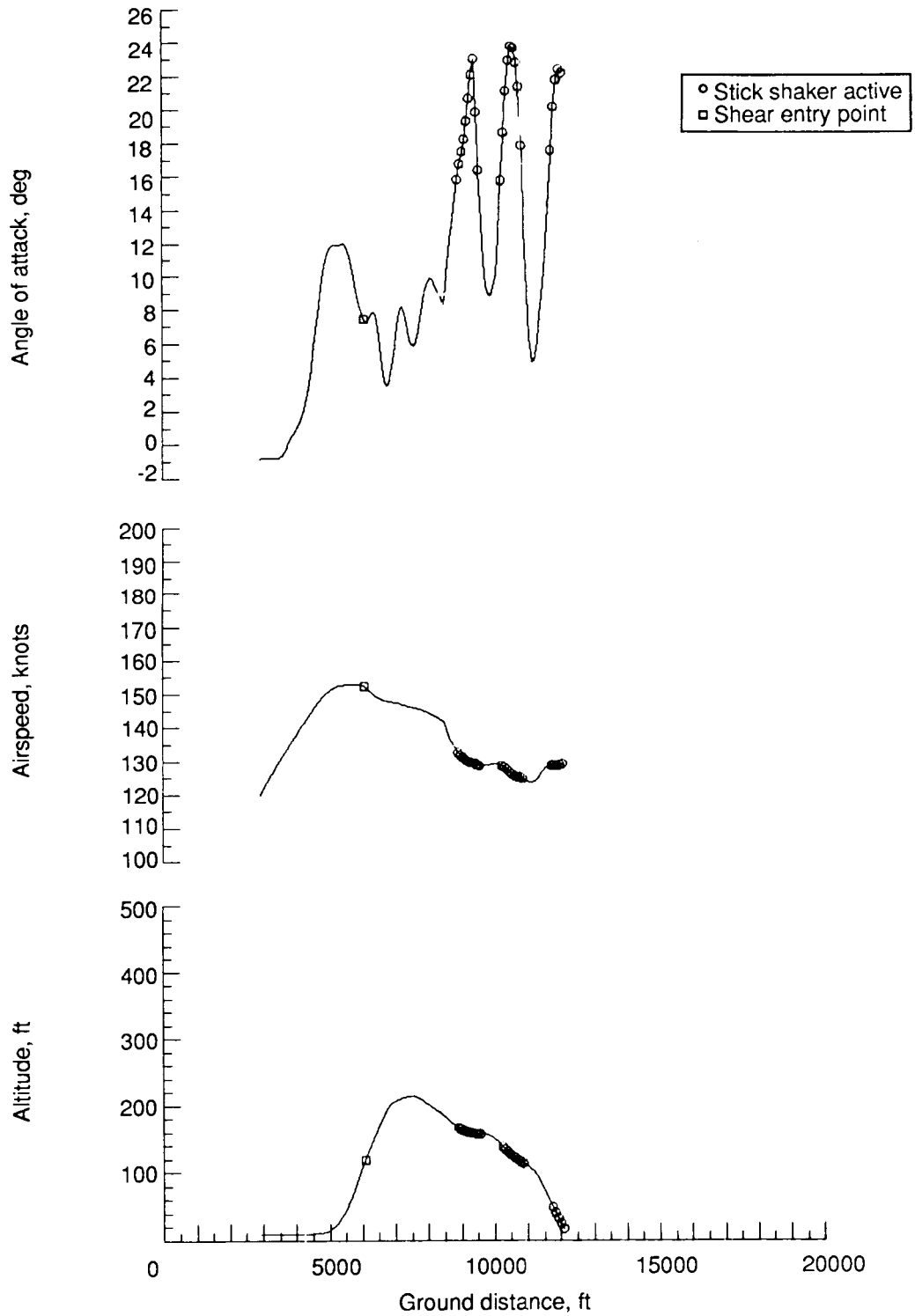


(a) Altitude, airspeed, and angle of attack.

Figure 13. Recovery from shear B1.30 with flight-path guidance.

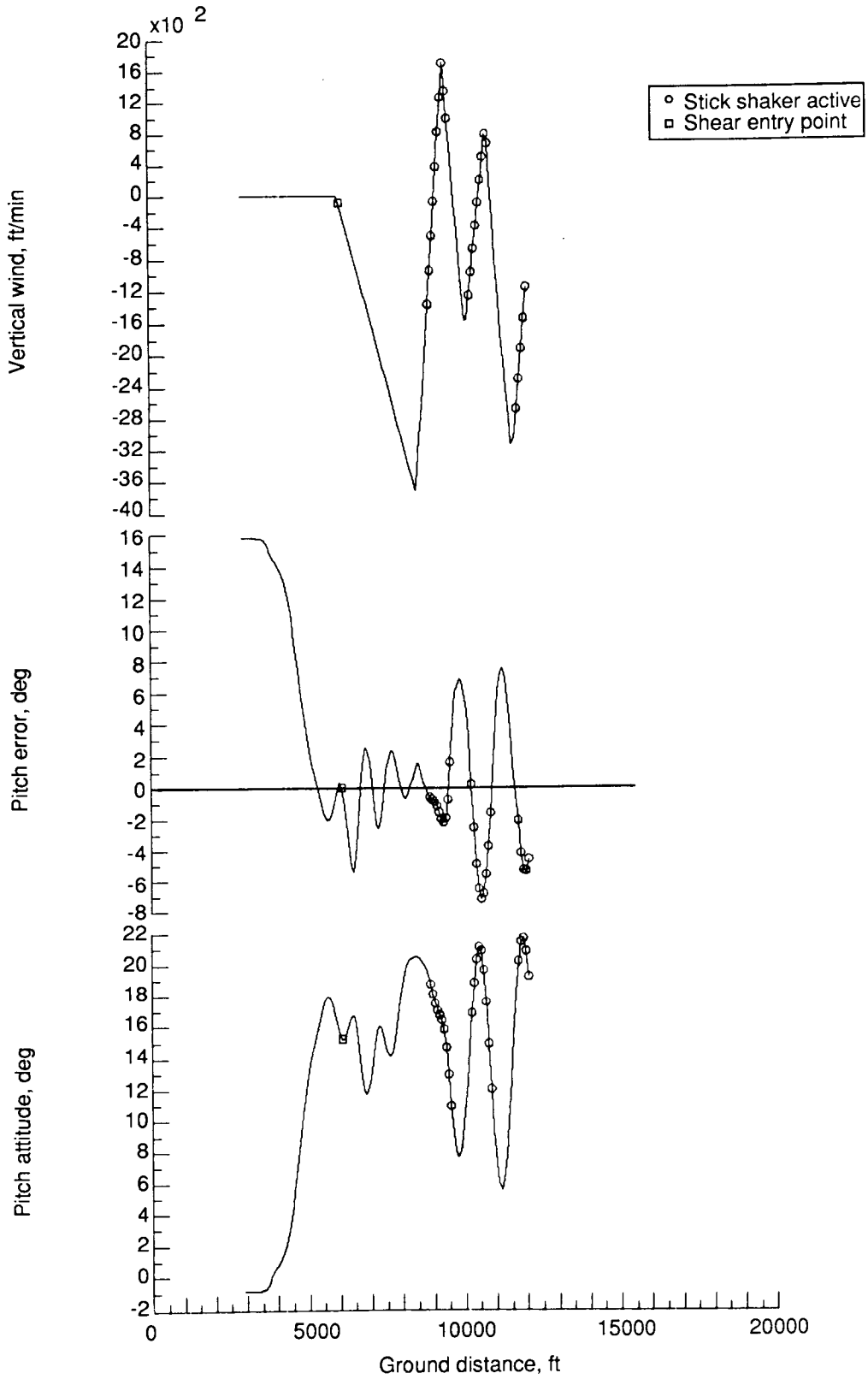


(b) Pitch attitude, pitch error, and vertical wind.

Figure 13. Concluded.

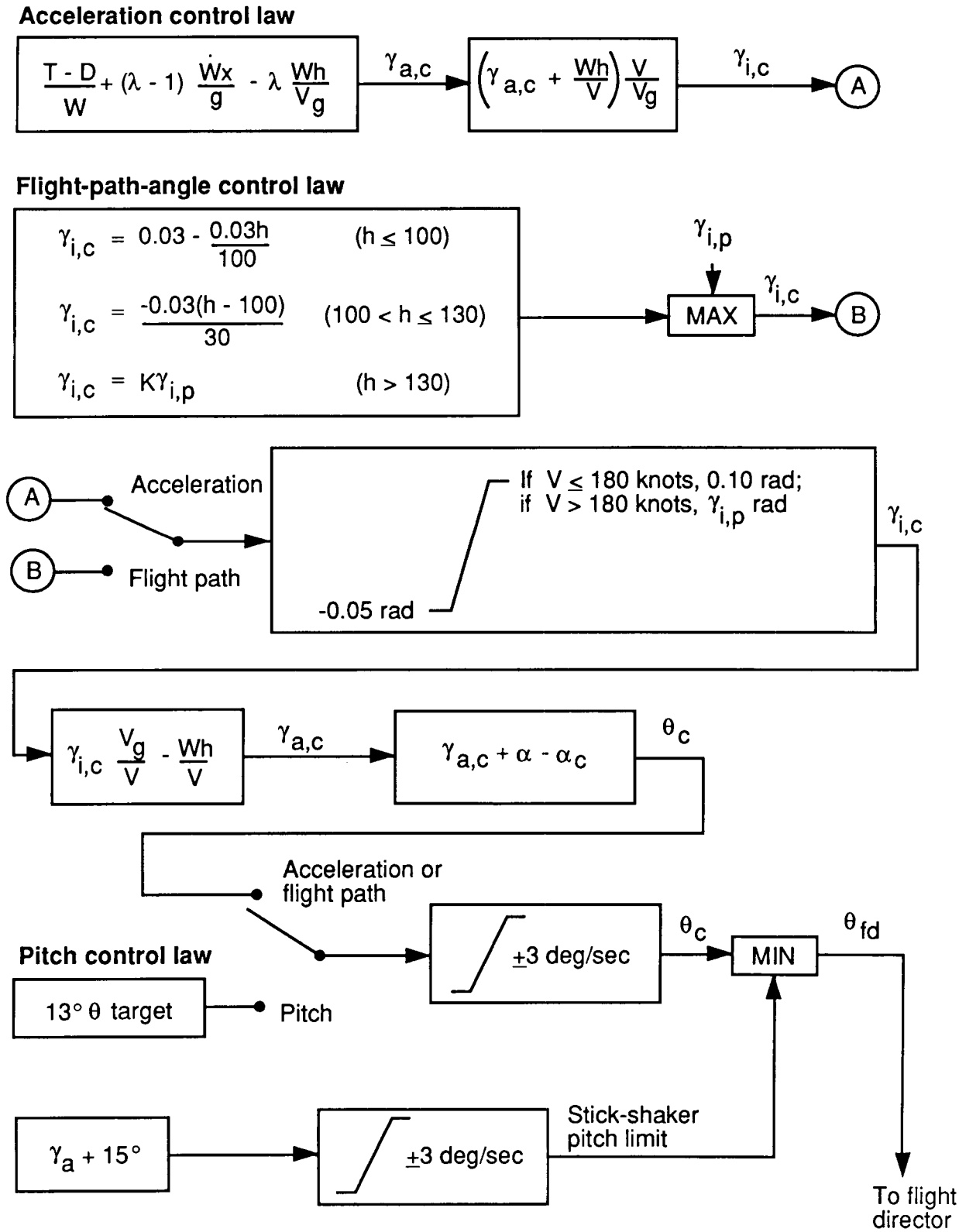


Figure 14. Flight-director pitch-axis command.

NASA
National Aeronautics and Space Administration

# Report Documentation Page

| 1. Report No. | 2. Government Accession No. | 3. Recipient's Catalog No. |
|---|---|---|
| NASA TP-2886<br>DOT/FAA/DS-89/06 | | |

| 4. Title and Subtitle | 5. Report Date |
|---|---|
| Piloted-Simulation Evaluation of Recovery Guidance for Microburst Wind Shear Encounters | March 1989 |
| | 6. Performing Organization Code |
| 7. Author(s) | 8. Performing Organization Report No. |
| David A. Hinton | L-16498 |
| 9. Performing Organization Name and Address | 10. Work Unit No. |
| NASA Langley Research Center<br>Hampton, VA 23665-5225 | 505-66-41 |
| | 11. Contract or Grant No. |
| 12. Sponsoring Agency Name and Address | 13. Type of Report and Period Covered |
| National Aeronautics and Space Administration<br>Washington, DC 20546-0001<br>and<br>Department of Transporation<br>Washington, DC 20590 | Technical Paper |
| | 14. Sponsoring Agency Code |

15. Supplementary Notes

Joint NASA and FAA report.

This research represents a portion of the work performed for the author's Master of Science degree from the George Washington University.

16. Abstract

Numerous air carrier accidents and incidents have resulted from encounters with the atmospheric wind shear associated with microburst phenomena, in some cases resulting in a heavy loss of life. An important issue in current wind shear research is how aircraft performance can be managed best during an inadvertent wind shear encounter. The goals of this study were (1) to develop techniques and guidance for maximizing the ability of an airplane to recover from microburst encounters following takeoff, (2) to develop an understanding of how theoretical predictions of wind shear recovery performance might be achieved in actual use, and (3) to gain insight into the piloting factors associated with recovery from microburst encounters. Three recovery strategies were implemented and tested in piloted simulation. Results show that a recovery strategy based on flying a flight-path-angle schedule produces an improved performance over constant pitch attitude or acceleration-based recovery techniques. The best recovery technique was initially counterintuitive to the pilots who participated in the study. Evidence indicated that the techniques required for flight through the turbulent vortex of a microburst may differ from the techniques being developed using classical, nonturbulent microburst models.

| 17. Key Words (Suggested by Authors(s)) | 18. Distribution Statement |
|---|---|
| Microburst situation<br>Flight-recovery guidance<br>Piloted simulation<br>Wind shear encounter | Unclassified—Unlimited<br><br>Subject Category 06 |

| 19. Security Classif. (of this report) | 20. Security Classif. (of this page) | 21. No. of Pages | 22. Price |
|---|---|---|---|
| Unclassified | Unclassified | 55 | A04 |



For sale by the National Technical Information Service, Springfield, Virginia 22161-2171